CHALMERS

A study of MIMO precoding algorithm in WCDMA uplink

Master's Thesis in Signals and Systems

Sheng Huang & Mengbai Tao

Department of Signals & Systems
Communication Engineering
Chalmers University of Technology
Gothenburg, Sweden 2014
Master's Thesis EX044/2014

Abstract

With rapidly increasing demand in high-speed data transmission, Multiple-Input Multiple-Output (MIMO) techniques are widely used in current communication networks, like Wideband Code Division Multiple Access (WCDMA). MIMO in downlink of WCDMA has been studied for a long time, while in WCDMA uplink, the specification of how to choose precoder is still not defined yet. Precoding is an essential element in MIMO, aiming at mitigating interference between different data streams that are sequences of digitally coded signals. Currently, a MIMO system suffer from two problems regarding precoding. Since channel information is needed for the precoding algorithm, one problem then is that it is difficult to model the channel characteristics in a frequency selective channel. The other problem is that only limited feedback is applicable in real system, since the cost of feedback overhead is far larger than the benefits from precoding if full channel information needs to be sent to the transmitter. The objective of this thesis is to investigate the maximum potential gain in the required Signal-to-Noise Ratio (SNR) range for a given Block Error Rate (BLER) by using precoding and selecting a suitable precoding algorithm in the case of limited feedback in the WCDMA uplink.

The maximum potential gain of precoding is considerable (1.2 dB at 0.5 BLER compared to a fixed precoder) in the case of limited feedback according to our simulations. By applying the proposed closest-to-SVD (CSVD) algorithm, 0.6 dB gain and 1 dB gain can be achieved for total stream and the primary stream, respectively, when ideal channel estimation is assumed. It is worth to point out that precoding alone can not mitigate crosstalk completely. Suitable channel equalization needs to be implemented together with precoding in order to further decrease the impact of crosstalk in MIMO. The performance of precoding depends largely on the reliability of the channel estimation as well. Thus, channel estimation needs to be more reliable in order to implement a good precoding algorithm in a commercial communication system, which on the other hand will cost more overhead and increase the system complexity. Hence, a trade-off should be made regarding the gain obtained from precoding and the complexity of the algorithm.

Keywords: MIMO, precoding, SVD, uplink, WCDMA

Acknowledgements

This thesis opportunity we had with Ericsson was a great chance for learning and professional development. Therefore, we would like to express special thanks of gratitude to the thesis proposer Krister Norlund, manager Ulf Lindgren and examiner Tommy Svensson, who gave us the golden opportunity to do this wonderful project.

We express our deepest thanks to our supervisors at Ericsson, Oskar Arvidsson Tjäder and Peter Hammarberg, for taking part in useful decisions and giving necessary advices and guidances and arranged all facilities to make our life easier, patiently and consistently. It is hard to imagine how can we come through the troubles we met without the help.

We would like to choose this moment to gratefully acknowledge the help from Tilak Rajesh Lakshmana, our supervisor from Chalmers. More than timely communications, he reviewed our report for a couple of times, giving out massive valuable comments, which improved the quality of our report largely from the very first version.

Thanks to our thesis colleagues Andreas Theodorakopoulos and Shijia Liu, for sharing knowledge with us.

Thanks to Anders Hansson for the technical help. Thanks to all the people who offered us help.

Sheng Huang and Mengbai Tao, Gothenburg, 2014-7-14

"Good judgment comes from experience, and experience comes from bad judgment"
— *Rita Mae Brown, including this quote in her book "Sudden Death"*

Contents

1

Introduction

Cellular communications systems are evolving from the early First-Generation (1G), Second-Generation (2G) to the upcoming Fifth-Generation (5G). The 1G systems are primarily comprised of voice-oriented analog cellular cordless telephones. One example is the Nordic Mobile Telephone (NMT) system [1]. The 2G wireless networks are also voice-oriented digital cellular systems. The most successful 2G voice-oriented digital cellular system is the Global System for Mobile communication (GSM) system. In the Third-Generation (3G) networks, the digital voice services are integrated with a variety of packet-switched data services in a unified network. The most widely used 3G networks is the Wideband Code Division Multiple Access (WCDMA) system. The Forth-Generation (4G) systems are completely packet-oriented, even for voice data. One example is the long Term Evolution (LTE) Advanced. The 5G systems need very high carrier frequencies with massive bandwidths, extreme densities of base stations and devices, and unprecedented numbers of antennas [2]. It will be a paradigm shift compared to previous four generations. To conclude, the trends of communication systems are from analog (1G) to digital (2G, ...), from voice-oriented (1G, 2G, 3G) to packet-oriented (3G, 4G, ...) and from low carrier frequencies with narrow bandwidth to high carrier frequencies with wide bandwidth.

Currently, with a rapidly increasing trend of video on demand traffic like YouTube, on-line games like Minecraft and streaming video/audio like Netflix and Spotify [2], there is a need for smart and efficient communication systems in terms of power and spectrum. Since spectrum is expensive and limited, it is essential to use spectrum more efficiently. There are a variety of methods to increase spectral efficiency, for example, using a higher order modulation scheme. Multiple antenna is an alternative technique. In this thesis, we will focus on a Multiple-Input Multiple-Output (MIMO) technique in the WCDMA standard.

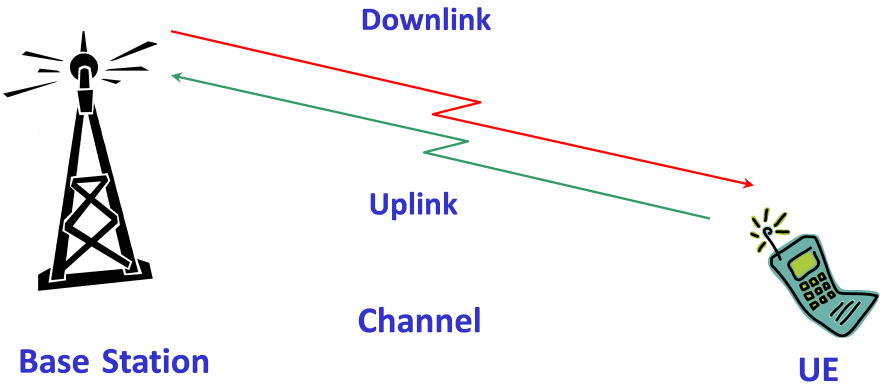

Figure 1.1: An example of a SISO model comprising a base station and a UE. The link from the UE to the base station is called uplink and that from the base station to the UE is called downlink.

1.1 Background of cellular communications with MIMO

A simplest form of a radio link can be defined as a Single-Input Single-Output (SISO) radio channel that employs a single transmit antenna and a single receive antenna. One example of a SISO system contains a base station and a User Equipment (UE) (a mobile phone, a laptop, etc.) as shown in figure 1.1. The transmission from the UE to the base station is called the Uplink (UL), while that from the base station to the UE is called the Downlink (DL). This basic physical model widely exists in the current telecommunication systems, e.g., 2G, 3G and 4G of mobile telecommunications technology networks.

The WCDMA technology is the most widely adopted 3G air interface. It is standardized by the Third Generation Partnership Project (3GPP) [3], which is a joint standardization project with bodies from Europe, Japan, Korea, the USA and China. Comparing with Interim Standard 95 (IS-95) that uses the Code Division Multiple Access (CDMA) technique, WCDMA users share a larger bandwidth and benefit from a much faster transmission speed. The maximum data rate can reach up to 42 Mbits/s with MIMO using single carrier in the downlink and 11 Mbits/s in the uplink [4]. However, as the need for higher data rates keeps increasing, modifications are needed in the uplink to achieve better throughput.

Currently there are two main methods that has been discussed in 3GPP for reaching that objective without using more than one carrier frequency: either utilize a higher modulation or/and use MIMO. A MIMO propagation channel is formed when multiple antennas are used at both transmitter and receiver. With additional antennas, multiple data streams can be sent and received. Hence, data rates can be increased significantly. As MIMO is already standardized for the downlink of WCDMA [5], it is logical to consider implementation of MIMO in the uplink to match the data rate in the downlink.

The performance of the WCDMA system is interference limited as the same frequency bandwidth or time duration is shared among users. Thus, adding more data streams introduces more interference that on the other hand limits the MIMO implementation in reality. It is necessary to have some mechanisms to limit the interference.

Precoding, a key element of MIMO techniques, is one way to mitigate the interference between different data streams. It is a generalization of beamforming that can support transmission for multiple streams in multi-antenna communication systems. Beamforming is a powerful technique to increase the link signal-to-noise ratio (SNR) through focusing the energy into desired direction. It is achieved when the transmit antennas are appropriately weighted in gain and phase for each transmission stream. In the case of multiple data streams, precoding generally combines the streams in orthogonal directions using weighting matrices according to the channel distribution. With channel status fully known at the transmitter and receiver, interference between different data streams could be limited by using a suitable precoding algorithm, resulting in higher data throughput [6].

1.2 The problem of MIMO precoding

Currently there are a number of research achievements in precoding algorithm studies [7, 8, 9]. However, most of these are based on the flat-fading assumption, i.e., similar fading characteristic for different frequency components of the signal. As a wideband transmission signal likely suffers a frequency-selective channel that gives different characteristics among frequency signal components, the methods mentioned above are inapplicable in WCDMA. Some other researchers stated methods that can solve the frequency-selective problem [11, 12]. Nevertheless, those methods are usually too complex to be implemented in practical system.

Another problem is the additional overhead caused by extra information feedback in a real MIMO system. In wireless communications, channel state information (CSI) refers to channel properties of a communication link that represents the combined effect of scattering, fading, power decay with the distance, etc. in a channel. Considering an uplink scenario in frequency division duplex (FDD) case, after the CSI is estimated at the base station, it then needs to be fed back to the UE through a downlink in order to calculate the precoding weights. The requirement of CSI feedback increases by two times of the number of transmit/receive antennas because for complex channel, both phase and amplitude needs to be estimated. On the other hand, the capacity of the channel just grows linearly with the number of antennas in an ideal case when perfect channel state information is known at both transmitter and receiver [13]. For instance, for a complex two-transmit and two-receive matrix channel, there are 8 parameters to be quantized every time when the channel changes (2×number of antennas) compared with only 1 parameter needed for fast power control in a single antenna link scenario. As a result, it is not efficient to have full channel information as feedback.

To reduce the complexity and overhead, in a practical system, a predefined codebook is used, which is a collection of precoding matrices. These matrices are quantized

in WCDMA, as defined by 3GPP. In the case of uplink, instead of sending an entire precoding matrix, a precoding index will be sent to the UE from the base station that denotes which matrix should be picked. Hence, how to select the precoding index becomes a key issue.

1.3 Methods for evaluation of precoding scheme

In this thesis, we address a scenario of 2×2 (2 transmit antennas and 2 receive antennas) Single User MIMO (SU-MIMO) uplink in WCDMA and investigate suitable precoding algorithms. Precoding schemes are designed in the UE to limit inter-stream-interference. Different algorithms that apply to calculate the precoding index are evaluated by performance of required Signal to Noise Ratio (SNR) for a given total Block Error Rate (BLER). A method of precoding index calculation that improves the performance of the system is proposed.

The simulator was built using IT++ [14], which is a C++ library of mathematical, signal processing and communication classes and functions. SNR versus BLER is the metric we used to evaluate the system throughput, as a block error will reduce the data rate. Results are obtained under two conditions: unlimited feedback condition, which means full channel information is known at the UE, or limited feedback condition, which means that the knowledge of channel information at the UE is limited. In this thesis, we focus on finding an algorithm that calculates precoding index and provides better BLER performance in a relatively low SNR range with unlimited feedback, and then different methods are tested for approaching this algorithm in a limited feedback condition.

1.4 Outline of this thesis

In this report, some key elements of WCDMA and MIMO theory are introduced in chapter 2, followed by some main specifications of the WCDMA standard and description of the simulator in chapter 3. Algorithms that are used to calculate the precoding index are investigated and simulation results are shown in chapter 4. Finally, conclusions and potential future research work are given in chapter 5.

2

WCDMA and MIMO theory

In this chapter, two essential techniques that are applied in our simulation model are described: WCDMA and MIMO. In the first section, some key components of WCDMA are introduced, including spread spectrum, Tapped Delay Line (TDL) channel model, channel estimation and channel equalization. In the Multiple antennas theory section, three different properties of MIMO are presented: beamforming, spatial diversity and spatial multiplexing. Then two precoding methods, channel inversion and Singular Value Decomposition (SVD), are described. An analysis of the case of limited feedback in precoding is presented in the end.

2.1 Introduction to WCDMA

WCDMA is a standard that uses Direct-Sequence Spread Spectrum (DSSS) based Direct-Sequence CDMA (DS-CDMA). Currently there are mainly three types of multiple access methods that share the time-frequency resources: Frequency Division Multiple Access (FDMA), Time-Division Multiple-Access (TDMA) and CDMA. Defining a digitally coded signal sequence as a data stream, in FDMA, data streams are allocated on different frequency band, and in TDMA, data streams are allocated to different time slots. Unlike those two methods, the same time and spectrum is used by all data streams in CDMA. Different CDMA data streams are separated by using different codes.

This section firstly introduces the DSSS method as the basis of WCDMA, with a description of the corresponding channel model following. Channel equalization is briefly described and a special kind of receiver structure called Rake receiver is put forward.

2.1.1 Spread spectrum

WCDMA is based on the DSSS method. Like all the other spread spectrum methods, DSSS spreads a user signal into a wider frequency band using specific codes. It is done by multiplying the data stream with a pre-defined sequence, i.e., spreading code sequence.

A simple model is shown in figure 2.1. Similar to the definition in [15], assuming the kth data stream Binary Phase Shift Keying (BPSK) modulated symbol sequence with length I is $\mathbf{m}_k(t) = [m_{k,1}, m_{k,2}, \cdots, m_{k,i}, \cdots, m_{k,I}]$, the ith data symbol in this sequence is $m_{k,i}(t)$. Before passing through the channel, it will be multiplied with a spreading code sequence $a(t)$, i.e.,

$$s_{k,i}(t) = m_{k,i}(t)a_{k,i}(t). \tag{2.1}$$

This process is called spreading. The spreading code sequence can be written as

$$a_{k,i}(t) = \frac{1}{\sqrt{N}} \sum_{l=1}^{N} c_{k,i}(l) p_{\text{rect}}(t - lT_c), \tag{2.2}$$

where $c_{k,i}(l)$ is called a chip. It belongs to a set of chips, $\{c_{k,i}(l)\}_{l=1}^{N}$. The chip duration T_c must be shorter than a symbol duration T_s, hence, a symbol will be spread into several chips. The ratio $N = T_s/T_c$ is called Spreading Factor (SF). Normally, SF should be chosen larger than four [3], which means there will be at least four chips representing one symbol. $p_{\text{rect}}(t)$ is corresponding to a rectangular pulse, i.e.,

$$p_{\text{rect}}(t) = \begin{cases} 1, & |t| \leq \frac{T_c}{2} \\ 0, & \text{otherwise.} \end{cases} \tag{2.3}$$

This function $p_{\text{rect}}(t)$ can be replaced by other kinds of pulse shape functions $p(t)$, e.g., an RRC pulse. In that case, the spreading code sequence $a_{k,i}(t)$ will become a spreading waveform.

At the receiver side, the received signal will be multiplied with the same spreading sequence with conjugated pulse shape, and integrated with the corresponding symbol time. This process is called despreading. Denoting the received signal for the ith symbol as $y_{k,i}(t)$, the despreading process can be written as

$$r_{k,i}(t) = \int_{-\infty}^{\infty} y_{k,i}(\tau) a_{k,i}^{*}(\tau - t) d\tau. \tag{2.4}$$

where the superscript "$*$" stands for the complex conjugate. The $r_{k,i}(t)$ stands for the despread value corresponding to the transmitted symbol i. The despreading integration

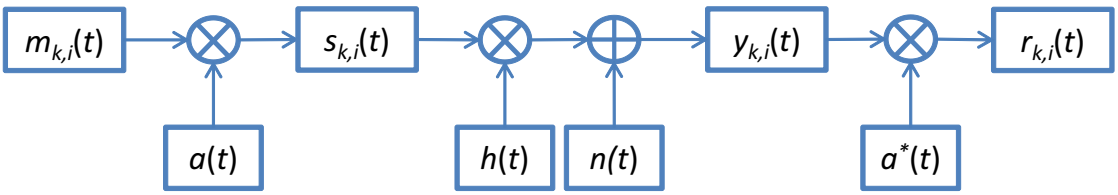

Figure 2.1: A simple block diagram of spread spectrum transmission link. Modulated symbols are firstly spread, and then sent to the one-tap channel. At the receiver, the signal is despread and then symbols are recovered.

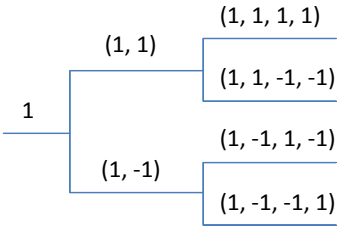

Figure 2.2: The picture shows three levels of a channelization code tree. Each code is orthogonal to all the codes on the other branches.

gives a spreading gain. The larger SF is selected, the larger spreading gain will be achieved. Hence, the receiver Signal-to-Interference-plus-Noise Ratio (SINR) is improved [3].

In order to perform a better data stripping from a single source, the spreading codes must be orthogonal, i.e.,

$$\mathbf{c}_k^H \mathbf{c}_l = 0, \quad k \neq l, \tag{2.5}$$

where $\mathbf{c}_k$ includes N chips, $\mathbf{c}_k = [c_k(1), c_k(2), \cdots, c_k(N)]$. The superscript "$H$" denotes the Hermitian transpose (conjugate transpose). This kind of code is called a channelization code. A channelization code should be selected inside an Orthogonal Variable Spreading Factor (OVSF) generated channelization code tree (see figure 2.2), so that no interference is introduced by the spreading process. Hence, for the kth and the lth data streams, after despread by code $\mathbf{c}_k$, the desired symbols from stream k are recovered and the other data stream l is thus suppressed.

2.1.2 Transmission channel model

Typically, a time-invariant transmission has the following expression

$$y(t) = hs(t) + n(t), \tag{2.6}$$

where h stands for the channel coefficient, which is a constant, and $n(t)$ stands for the instantaneous thermal noise that usually characterized as an Additive White Gaussian Noise (AWGN). If the channel is not stable through time, the equation will become

$$y(t) = h(t)s(t) + n(t), \tag{2.7}$$

where channel coefficient $h(t)$ is a function of time.

In reality, a radio channel is composed of several copies of delayed original signal. These copies, or multipath components, come from the reflection, refraction or diffraction from buildings, mountains or other objects, which often resulting in amplitude change, phase shift and time delay [10]. This kind of channel is modeled as a Tapped Delay Line (TDL) channel (see figure 2.3).

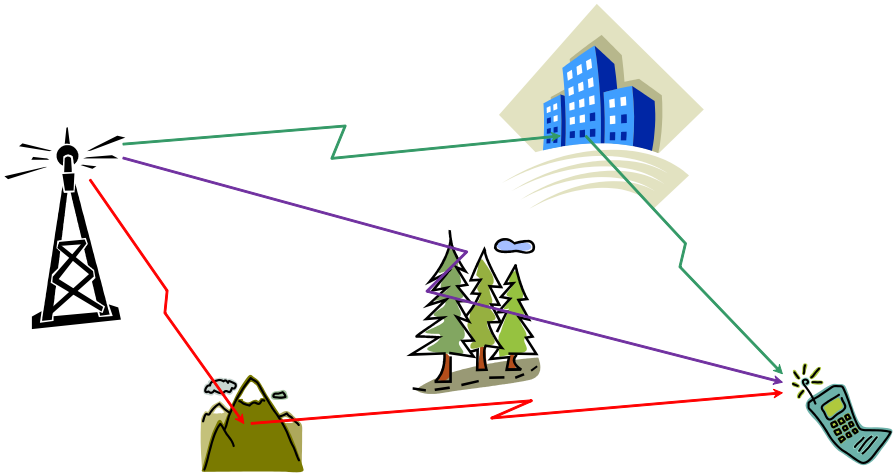

Figure 2.3: This picture sketches a TDL channel. Multipath components come from the reflection, refraction or diffraction from buildings, mountains or other objects.

TDL channel impulse response can be considered as a sum of taps with different scaling and phase rotating characteristics, i.e.,

$$h(t,\tau) = \sum_{l=1}^{L} h_l(t)\delta(\tau - \tau_l), \tag{2.8}$$

where L stands for the total number of taps, and t_l stands for the time delay corresponding to the lth tap [15]. $\delta(\tau)$ stands for the Dirac delta function. Each tap stands for a multipath component, which follows a Rayleigh distribution. Hence, eq. (2.6) becomes

$$y(t) = \int_{-\infty}^{\infty} h(t,\tau)s(t-\tau)d\tau + n(t) = \sum_{l=1}^{L} h_l(t)s(t-\tau_l) + n(t). \tag{2.9}$$

Figure 2.4 shows a TDL channel characteristic. It is obvious that the channel coefficient $h(t,\tau)$ of a TDL channel is time varying. However, within a time interval, the channel changes can be ignored and the coefficient $h(t,\tau)$ can be considered as a constant h. This time interval is called coherence time. Thus, a signal with a duration that is shorter than the coherence time is described as passing through a slow-fading channel, while the other signals that cannot fulfill this condition are described as passing through a fast-fading channel.

Similarly, a TDL channel characteristic varies in the frequency domain. Coherence bandwidth is defined as a frequency range that the channel changes can be ignored. A signal that has a bandwidth narrower than the coherence bandwidth is described as passing through a flat-fading channel. On the contrary, if a signal has a larger bandwidth than the coherence bandwidth, the characteristics that different frequency components see can be quite different. Hence, this channel is described as a frequency-selective channel.

By implementing spreading, a WCDMA signal will be spread into a wider spectrum band than the original signal. As a drawback, in the case of high speed transmission with relatively low spreading factor values, the signal will suffer more from a frequency-selective channel, which influences the system performance greatly.

2.1.3 Channel estimation and equalization

Channel estimation and equalization are implemented to remove the effect of the channel. The estimation is achieved using a known pilot sequence. Denoting the transmitted complex pilot as $s_p(t)$, the received signal will have the following format

$$\tilde{y}_p(t) = \sum_{l=1}^{L} h(t)s_p(t-\tau_l) + n(t). \tag{2.10}$$

Considering for a single sample of the pilot signal $s_p(q)$, the eq. (2.10) becomes

$$\tilde{y}_p(q) = \sum_{l=1}^{L} h(q)s_p(q-\tau_l) + n(q). \tag{2.11}$$

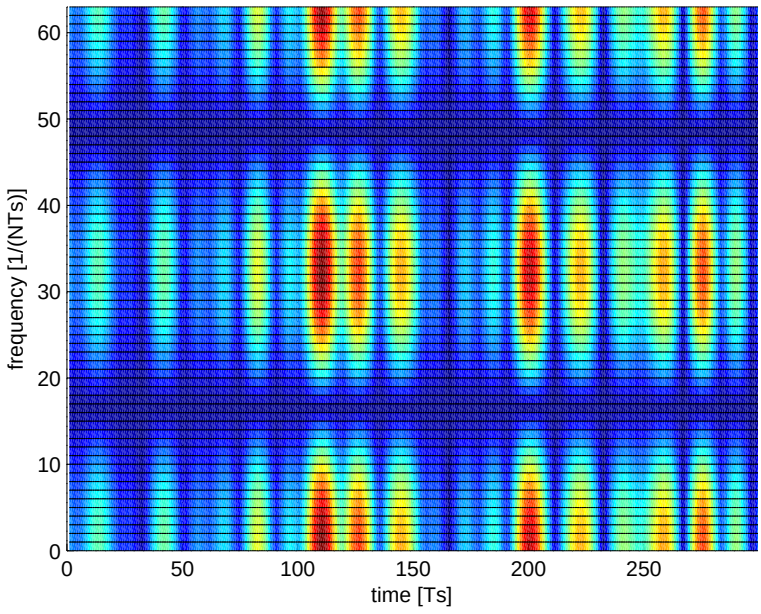

Figure 2.4: This picture shows a typical TDL channel realization. Cool colored regions have large channel attenuation, which means the signal passing through will suffer a deep fading.

For the tap l, the estimation value can achieved by implementing a division

$$\hat{h}_l(q) = \frac{\tilde{y}_p(q)}{s_p(q - \tau_l)}. \tag{2.12}$$

Thus, the channel estimation result is

$$\hat{h}_l(q) = h_l(q) + \varepsilon_l(q), \tag{2.13}$$

where $\varepsilon(q)$ denotes the estimation error for the qth sample. For a certain time period, if the channel is slow-fading, an estimated coefficient value for a certain time period T can be achieved by averaging the estimated values among samples, i.e.,

$$\hat{h}_l = \frac{1}{Q} \sum_{q=1}^{Q} \frac{\tilde{y}_p(q)}{s_p(q - \tau_l)}. \tag{2.14}$$

In continuous time domain, eq. (2.14) becomes

$$\hat{h}_l = \frac{1}{T} \int_0^T \frac{\tilde{y}_p(\tau)}{s_p(\tau - \tau_l)} d\tau. \tag{2.15}$$

Multiplying the complex conjugate of $\hat{h}$ to the received signal will recover an estimate of the transmitted signal from the corresponding tap, i.e.,

$$\hat{s}_l(t) = \hat{h}_l^* \tilde{y}(t), \tag{2.16}$$

which is called equalization. It can be performed on either chip level or symbol level, depending on the receiver structure [16].

Nevertheless, a frequency-selective channel cannot be simply modeled by one coefficient. Hence, in order to compensate for a frequency-selective channel, a more complex scheme is needed. One solution that is widely used is the Rake receiver [17].

2.1.4 Rake receiver

Basic Rake receiver

A Rake receiver is a multiple correlating receiver used in multipath transmissions, especially in WCDMA cellular systems. The time-shifted versions of original signals, which corresponds to the so-called fingers in the Rake receiver, are collected and combined in a certain way to improve the SNR. The delayed copies can be combined in such a way mainly because the multipath components are usually uncorrelated from each other when there are more than one chip propagation delay [10, 17].

The structure of a conventional rake receiver in WCDMA is illustrated in figure 2.5. Firstly, the channel impulse response is calculated by the correlators (each correlator acts as a matched filter) that correlate the received signal with a known sequence, e.g., a pilot.

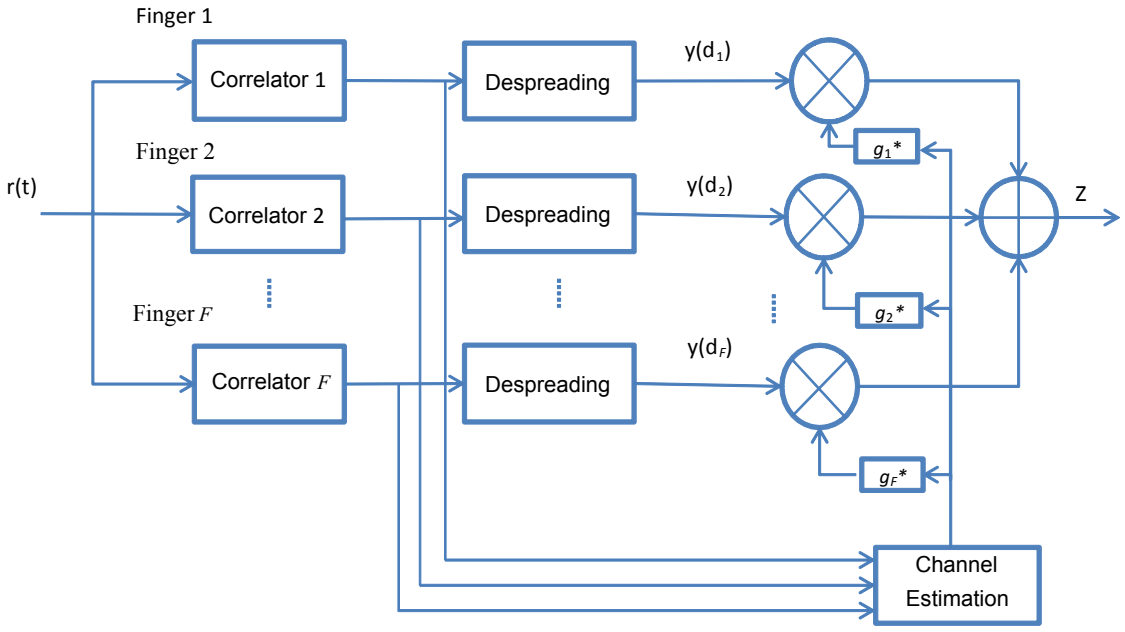

Figure 2.5: Rake receiver structure in CDMA. Basically, a rake receiver in WCDMA comprises of correlators, despreading and MRC.

Assuming perfect synchronization, the correlators will find correct starting positions for each finger and then down-sample the input sequence by a certain period. The fingers are located based on the delays obtained by the channel impulse response. Afterwards, despreading and possible descrambling are done for each finger. The channel estimation is implemented for each finger respectively. Adaptive channel estimation in this case is based on the known pilot symbols, which gives far better performance than that of using fixed channel coefficients in the presence of various channel conditions.

By applying Maximum Ratio Combining (MRC), a weighting matrix is multiplied to each finger elements according to the estimated complex-valued channel gain. Hence, compensation is made for channel phase shift. The signal is weighted by a factor which is proportional to the signal strength to ensure the finger with the highest weight dominates the received signal. In addition, the effect of additional noise is also decreased, which is further suppressed by channel coding.

Recalling eq. (2.8), the multipath propagation channel is characterized by the base-band equivalent impulse response. Assuming perfect channel estimation, the received symbols $\mathbf{z}$ are given by

$$\mathbf{z} = \mathbf{g}^H \mathbf{r}, \tag{2.17}$$

where vector $\mathbf{r} \in \mathbb{C}^{1\times I}$ is the received symbol sequence with a length of I. $\mathbf{g} \in \mathbb{C}^{L\times 1}$ is a vector that contains L complex combining weights that are used in the MRC based on Maximum Likelyhood (ML). Then in the Rake receiver,

$$\mathbf{g} = \mathbf{R}^{-1}\hat{\mathbf{h}}, \tag{2.18}$$

where $\mathbf{R} \in \mathbb{C}^{L \times L}$ is the impairment correlation matrix with a dimension $L \times L$ and $\hat{\mathbf{h}}$ is the channel estimation.

Considering a simple example of a TDL channel with two taps, the $\mathbf{R}$ is represented as

$$\mathbf{R} = \begin{bmatrix} |\hat{h}_1|^2 & 0 \\ 0 & |\hat{h}_0|^2 \end{bmatrix}, \tag{2.19}$$

and

$$\hat{\mathbf{h}} = [\hat{h}_0 \;\; \hat{h}_1]^T, \tag{2.20}$$

where the superscript "T" stands for the matrix transpose operation. Then, the resulting weight matrix can be expressed as

$$\mathbf{z} = \mathbf{g}^H \mathbf{r} = \begin{bmatrix} \frac{\hat{h}_0}{|\hat{h}_1|^2} & \frac{\hat{h}_1}{|\hat{h}_0|^2} \end{bmatrix}^H \mathbf{r}. \tag{2.21}$$

Assuming $|\hat{h}_0|^2 < |\hat{h}_1|^2$, the first finger has more interference on the received signal, which is reflected in the resulting weight.

Generalized Rake receiver

For WCDMA, a Generalized Rake (G-Rake) receiver can be applied for interference suppression and multipath mitigation. The interference of different fingers is modeled as colored, while Gaussian noise is used to account for multipath dispersion and pulse shaping [15]. Compared to conventional Rake receivers, the G-Rake receivers have more fingers (beyond the number of multipath components) and different combining weights. Maximum likelihood formulation are used to calculate the weights. Bit Error Rate (BER) and BLER are usually applied to evaluate the performance and optimize the finger placement.

Assuming there are L taps in the channel and F fingers in the G-Rake receiver, a suitable choice for F is $L < F \leq 2L$ fingers according to numerical results [15]. A simple strategy to place the fingers is to put L fingers in the multipath components to collect energy and the remaining $F - L$ fingers are placed based on the strongest taps of the inverse channel filter to suppress the interference. The main idea to implement interference suppression in G-Rake is presented by the following formula

$$\mathbf{g} = \mathbf{R}_u^{-1} \hat{\mathbf{h}}. \tag{2.22}$$

$\mathbf{R}_u = \mathrm{E}\{\mathbf{u}\mathbf{u}^H\}$, where $\mathrm{E}\{\cdot\}$ stands for the expected value. Vector $\mathbf{u}$ models the overall noise, including noise and interference, that is assumed to be a vector of zero mean complex-valued Gaussian noise [15]. $\hat{\mathbf{h}}$ is a complex-valued vector of the estimated channel. $\mathbf{g}$ is formed as a column vector with a length equal to the number of fingers, and each containing element stands for the MRC combining weight for the corresponding finger.

2.2 Multiple antennas theory

It has been widely acknowledged that MIMO techniques can be utilized to increase the spectrum efficiency as well as peak data rate [18]. Different data can be sent from different antennas simultaneously, hence the data rate can in theory be increased by adding more antennas. In addition, given that the antennas are spatially separated sufficiently, different channel characters can be seen by different transmissions. Hence, it becomes more unlikely for the entire link to suffer from deep fading.

2.2.1 MIMO techniques overview

A general MIMO system model is shown in figure 2.6. Regarding a $M \times N$ MIMO system, several data streams are sent out through channel $\mathbf{H} = [\mathbf{h}_1, \mathbf{h}_2, \cdots, \mathbf{h}_m, \cdots, \mathbf{h}_M]$, where $\mathbf{h}_m = [h_{m1}, h_{m2}, \cdots, h_{mN}]^T$ stands for the channel seen by the signal transmitted from antenna m. Considering one single sample from each stream, the transmitted signal can be written as $\mathbf{s} = [s_1, s_2, \cdots, s_M]^T$. The receiver collects data from the antennas separately, which is shown as $\mathbf{y} = [y_1, y_2, \cdots, y_{\mathrm{N}}]^T$. The AWGN noise is denoted as $\mathbf{n} = [n_1, n_2, \cdots, n_n, \cdots, n_N]$, where each element $n_n \sim \mathcal{CN}(0, \sigma_a^2)$ is independent and identically distributed (i.i.d.) AWGN noise, and σ_a^2 stands for the noise variance. Hence, the model can be written as

$$\mathbf{y} = \mathbf{H}\mathbf{s} + \mathbf{n}. \tag{2.23}$$

There are other special cases, like the model that contains single transmitter antenna and several receiver antennas, corresponding to the terminology Single-Input Multiple-Output (SIMO), and the model that contains several transmitter antennas but only one receiver antenna, corresponding to the terminology Multiple-Input Single-Output (MISO). To fulfill different requirements of implementation, there are mainly three kind of techniques:

- Beamforming
- Spatial diversity
- Spatial multiplexing.

Beamforming

Beamforming techniques are well established since the 1960's, originating from the field of radar technology. However, intense research for wireless communication systems was not started until the 1990's [19].

The basic idea of beamforming is to use antenna arrays to transmit (and/or receive) signals from/to a certain direction. This is achieved by adjusting the phases of the radio frequency signals. Array gain can be achieved by focusing antenna patterns on a desired angle, e.g. towards Line Of Sight (LOS) or significant scatters. Thus, it improves the received SNR without increasing transmission power. This method is usually used in the

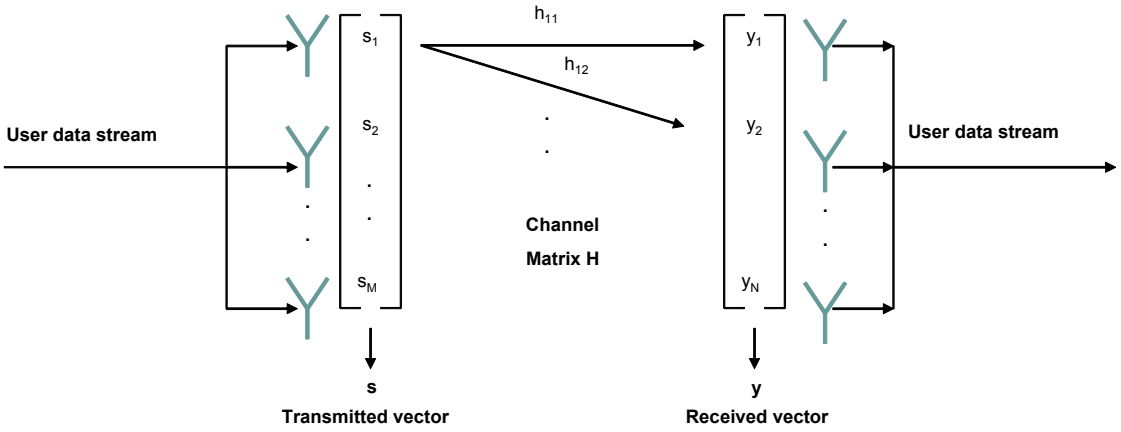

Figure 2.6: MIMO system model. User signal is split into M streams and sent to the channel. Receiver collects received signal from different antennas, and then send it for decoding.

scenarios where SNR is relatively low or there is a high requirement of data reliability. Beamforming can be used to limit interference as well.

Spatial diversity

Spatial diversity is another technique dealing with situations when SNR is low. Basically, there are two types of spatial diversity: receive diversity and transmit diversity.

If there are more than one receiver antennas involved in a wireless transmission link, receiver diversity can be achieved. Linear combining is used at the receiver after collecting the signal from different antennas. There are various combining strategies, e.g. Equal-Gain Combining (EGC), Selection combining (SC) and MRC [10].

Transmit diversity is achieved by appropriate preprocessing of transmitted redundant signals to enable coherent combining at the receiver. A well-known method called space-time coding can be applied [20] for that purpose. To perform a successful transmission in the transmit diversity model, channel knowledge is required solely at the receiver.

One of the assumptions behind spatial diversity techniques is that the redundant signal undergoes statistically independent fading. Hence, it requires a certain distance between antennas. This method improves the performance especially in the case of deep fading, giving a diversity gain.

Spatial multiplexing

The goal of spatial multiplexing techniques is to increase data rate by sending several data streams in parallel. Let us take an example that there are M antennas at the transmitter and N antennas at the receiver. At the transmitter side, the data sequence is split into M sub-sequences that are transmitted simultaneously using the same frequency band. The capacity of a MIMO system using multiplexing grows lin-

early with $\min(M, N)$. $N \geq M$ is strictly required [18]. At the receiver, the subsequences are detected and collected by interference cancellation algorithms, like Zero-Forcing (ZF)/Minimum-Mean-Squared-Error (MMSE) detectors [21], ML detectors and Interference Cancellation (IC) detectors [16], etc..

There is a trade-off between spectral efficiency (high data rates) and power efficiency (small error rates), given fixed bandwidth and transmission power [22]. Using multiple antenna techniques according to the transmission environment and Quality of Service (QoS) requirements can increase spectral efficiency while keeping error rates tolerable.

As MIMO multiplexing methods introduce extra data streams, for a specific stream, all the other streams are regarded as interference. In high SNR cases, the interference is much stronger than the noise. Hence, SINR becomes more significant than SNR.

2.2.2 Precoding

As mentioned in the chapter 1, precoding is generalized beamforming to support multiple streams transmission in a multi-antenna communication system through focusing the energy into desired direction. Its functionality is to mitigate the interference between different streams.

Figure 2.7 shows the role of precoding in a 2×2 MIMO system. Assuming two independent data streams are sent from the transmitter, after precoding, the two streams are mixed to each other with precoding weights and then transmitted from different antennas. Hence, beamforming is formed. In the receiver, the received data streams are decoded by using decoding methods that corresponds to the transmitter and channel condition. In the meantime, the feedback from the receiver about channel information through channel estimation will be sent to the transmitter to select the suitable precoder.

Precoding aims at maximizing the SINR and achieving a maximum channel capacity. According to [16], C_k, the capacity of the kth data stream, corresponds to

$$C_k = \log(1 + SINR_k), \tag{2.24}$$

where

$$SINR_k = \frac{\sigma_y^2}{MMSE_k} - 1. \tag{2.25}$$

In this equation, the σ_y^2 stands for the variance of the received signal power (including noise and interference), and $MMSE_k$ stands for the MMSE value of the kth data stream. Denoting the precoding matrix as $\mathbf{W}$, with precoding the transmission can be modeled as

$$\mathbf{y} = \mathbf{HWs} + \mathbf{n}. \tag{2.26}$$

Obviously, the optimal precoding matrix $\mathbf{W}$ that can maximize the sum-capacity of the streams satisfies an LMMSE expression [16], namely,

$$\mathbf{W}_{\text{opt}} = \arg\max_{\mathbf{W}} \left[\log \left(\prod_k \frac{\sigma_y^4}{MMSE_k} \right) \right]. \tag{2.27}$$

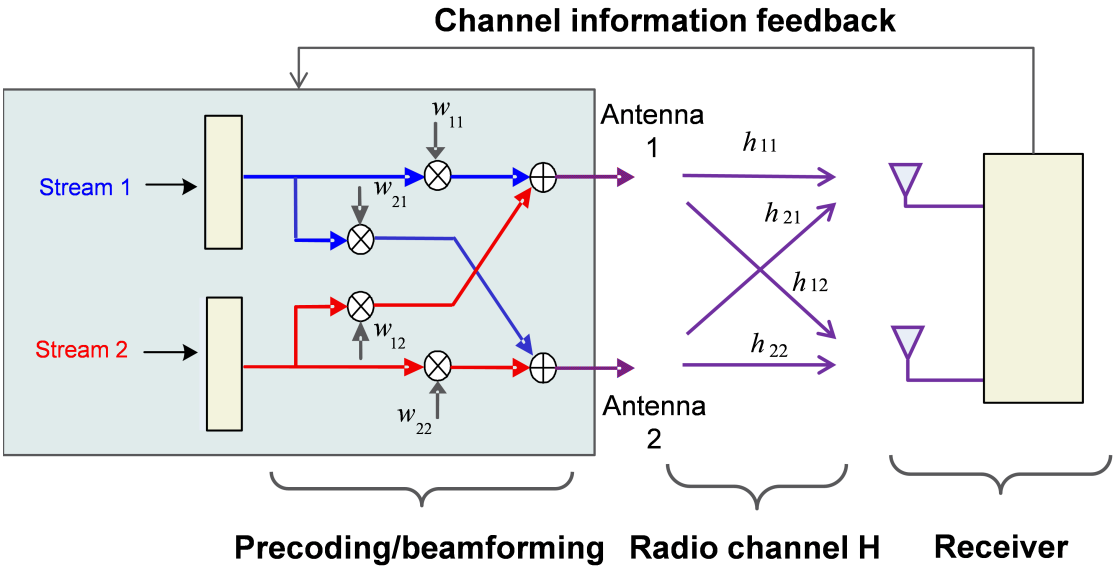

Figure 2.7: Precoding in 2 x 2 SU-MIMO

and

$$MMSE_k = \arg\min_{\mathbf{W}} \mathrm{tr}\{\mathrm{E}\{(\mathbf{z}_k - \mathbf{m}_k)(\mathbf{z}_k - \mathbf{m}_k)^T\}\}, \tag{2.28}$$

where $\mathbf{z}_k$ stands for the received symbols and $\mathbf{m}_k$ stands for the transmitted symbols.

Channel inversion precoding method

One method to calculate precoding matrix is to use the channel inversion method proposed in [23], which is the simplest scheme available regarding complexity. Recall the eq. (2.23), a 2×2 MIMO narrow band transmission system can be written as

$$\begin{bmatrix} y_1 \\ y_2 \end{bmatrix} = \begin{bmatrix} h_{11} & h_{21} \\ h_{12} & h_{22} \end{bmatrix} \begin{bmatrix} s_1 \\ s_2 \end{bmatrix} + \begin{bmatrix} n_1 \\ n_2 \end{bmatrix}. \tag{2.29}$$

Denote the precoding matrix as

$$\mathbf{W} = \begin{bmatrix} w_{11} & w_{21} \\ w_{12} & w_{22} \end{bmatrix}, \tag{2.30}$$

with precoding, the equation becomes

$$\begin{bmatrix} y_1 \\ y_2 \end{bmatrix} = \begin{bmatrix} h_{11} & h_{21} \\ h_{12} & h_{22} \end{bmatrix} \begin{bmatrix} w_{11} & w_{21} \\ w_{12} & w_{22} \end{bmatrix} \begin{bmatrix} s_1 \\ s_2 \end{bmatrix} + \begin{bmatrix} n_1 \\ n_2 \end{bmatrix}. \tag{2.31}$$

Theoretically, the inversion of the channel matrix $\mathbf{H}$ can be used as the precoding matrix, i.e.,

$$\mathbf{W} = \mathbf{H}^{-1}. \tag{2.32}$$

Hence, the system becomes

$$\begin{bmatrix} y_1 \\ y_2 \end{bmatrix} = \begin{bmatrix} 1 & 0 \\ 0 & 1 \end{bmatrix} \begin{bmatrix} s_1 \\ s_2 \end{bmatrix} + \begin{bmatrix} n_1 \\ n_2 \end{bmatrix} = \begin{bmatrix} s_1 \\ s_2 \end{bmatrix} + \begin{bmatrix} n_1 \\ n_2 \end{bmatrix}, \tag{2.33}$$

or equivalently written as

$$\mathbf{y} = \mathbf{I}_2\mathbf{s} + \mathbf{n} = \mathbf{s} + \mathbf{n}, \tag{2.34}$$

where $\mathbf{I}_2$ is a 2×2 identity matrix.

With a perfect channel inversion precoding, the signal can be considered as passing through two parallel SISO channels without interfering each other. However, the throughput in this case is limited and will not be improved when increasing the number of antennas, as proved in [7]. In addition, as a characteristic of matrix inversion operation, if a matrix contains very small elements, its inverse matrix will contain very big values. Hence, it is not power efficient in the case of deep fading.

SVD precoding method

A more well-known alternative is the Singular Value Decomposition (SVD) algorithm [10]. To implement this method, SVD is applied on the channel matrix, i.e.,

$$\mathbf{H} = \mathbf{U}\Sigma\mathbf{V}^{\mathrm{H}}, \tag{2.35}$$

where $\mathbf{U}$ and $\mathbf{V}$ are unitary matrices, i.e.,

$$\mathbf{U}^{\mathrm{H}} = \mathbf{U}^{-1}, \mathbf{V}^{\mathrm{H}} = \mathbf{V}^{-1}. \tag{2.36}$$

The matrix Σ is a diagonal matrix that has the same dimension as the channel matrix, and containing only non-negative real values. Those values are known as the singular values, which can be considered as the most significant channel characteristics. By choosing matrix $\mathbf{V}$ as the precoding matrix, i.e.,

$$\mathbf{W} = \mathbf{V}, \tag{2.37}$$

the system can be written as

$$\begin{aligned} \mathbf{y} &= \mathbf{HVs} + \mathbf{n} \\ &= \mathbf{U}\Sigma\mathbf{V}^{\mathrm{H}}\mathbf{Vs} + \mathbf{n} \\ &= \mathbf{U}\Sigma\mathbf{s} + \mathbf{n}. \end{aligned} \tag{2.38}$$

The cross talk can be mitigated by implementing a post-coding process at the receiver using the matrix $\mathbf{U}^{\mathrm{H}}$. Hence, the system becomes

$$\begin{aligned} \mathbf{y} &= \mathbf{U}^{\mathrm{H}}\mathbf{U}\Sigma\mathbf{s} + \mathbf{n} \\ &= \Sigma\mathbf{s} + \mathbf{n} \end{aligned} \tag{2.39}$$

In the case of 2×2 MIMO transmission, the eq. (2.39) can be written as

$$\begin{bmatrix} y_1 \\ y_2 \end{bmatrix} = \begin{bmatrix} \rho_{11} & 0 \\ 0 & \rho_{22} \end{bmatrix} \begin{bmatrix} s_1 \\ s_2 \end{bmatrix} + \begin{bmatrix} n_1 \\ n_2 \end{bmatrix}, \tag{2.40}$$

where ρ_{11} and ρ_{22} stand for the singular values. As a property of the SVD algorithm, there exists a relation that $\rho_{11} > \rho_{22}$. Hence, the complex channel has been decomposed into two parallel real channels, and the system can be considered as two parallel SISO communication links without inter-stream interference, theoretically.

In a wide band transmission system, the MIMO will suffer from the impact of the frequency-selective channel characteristic. To keep the consistency, for a 2×2 MIMO frequency-selective transmission we rewrite the formula (2.29) as following:

$$\begin{aligned} \mathbf{y} &= \mathbf{Hs} + \mathbf{n}, \\ \begin{bmatrix} \mathbf{y}_1 \\ \mathbf{y}_2 \end{bmatrix} &= \begin{bmatrix} \mathbf{h}_{11} & \mathbf{h}_{21} \\ \mathbf{h}_{12} & \mathbf{h}_{22} \end{bmatrix} \begin{bmatrix} s_1 \\ s_2 \end{bmatrix} + \begin{bmatrix} \mathbf{n}_1 \\ \mathbf{n}_2 \end{bmatrix}, \end{aligned} \tag{2.41}$$

where $\mathbf{h}_{mn}$ represent the channel characteristic seen by the signal transmitted from the mth transmitter antenna to the nth receiver antenna. Each element $\mathbf{h}_{mn}$ is a vector that contains the multipath coefficients, i.e., $\mathbf{h}_{mn} = [h_{mn,0}, h_{mn,1}, \cdots, h_{mn,l}, \cdots, h_{mn,L}]^T$ where L is the total number of taps. It is obvious that the channel matrix $\mathbf{H}$ becomes a $2L \times 2$ matrix and the output signal of channel $\mathbf{y}$ becomes a vector with length $2L$. Hence, the simple channel inversion cannot be implemented.

The SVD method is applicable on a non-square matrix, and gives out a 2×2 precoding matrix. Hence, the formula is formed as

$$\mathbf{H}_{2L\times 2} = \mathbf{U}_{2L\times 2L} \Sigma_{2L\times 2} \mathbf{V}^{\mathrm{H}}_{2\times 2}. \tag{2.42}$$

Using the similar procedure as in frequency flat-fading conditions, i.e., $\mathbf{V}$ is used for precoding and $\mathbf{U}^H$ is used for post coding, this channel can be decomposed into two independent channels and crosstalk can be completely avoided in theory.

Channel estimation with precoding

Considering a 2×2 MIMO transmission of the pilot $\mathbf{s}_p$, where

$$\mathbf{s}_p = [s_{p1} \;\; s_{p2}]^T, \tag{2.43}$$

the eq. (2.23) can be reconstructed as

$$\tilde{\mathbf{y}}_p = \mathbf{Hs}_p + \mathbf{n}. \tag{2.44}$$

Hence, the channel estimation process becomes

$$\begin{aligned} \hat{\mathbf{H}} &= \tilde{\mathbf{y}}_p \mathbf{s}_p^H, \\ &= \mathbf{H} + \varepsilon. \end{aligned} \tag{2.45}$$

While precoding is implemented, pilot is coded as well. Hence the eq. (2.44) becomes

$$\tilde{\mathbf{y}}_p = \mathbf{HWs}_p + \mathbf{n}. \tag{2.46}$$

In this case, the channel estimation will estimate the coded channel instead of the real channel, i.e.,

$$\hat{\mathbf{H}}_{\text{eff}} = \mathbf{HW} + \varepsilon. \tag{2.47}$$

The estimated channel $\hat{\mathbf{H}}_{\text{eff}}$ is called effective channel. To get the estimation values of the real channel, the precoder must be removed from the $\hat{\mathbf{H}}_{\text{eff}}$, i.e.,

$$\begin{aligned} \hat{\mathbf{H}} &= \hat{\mathbf{H}}_{\text{eff}}\mathbf{W}^{-1}, \\ &= \mathbf{H} + \varepsilon'. \end{aligned} \tag{2.48}$$

In a MIMO transmission procedure, eq. (2.48) is employed on the effective channel estimation matrix obtained from the previous pilot, so that estimation of the real channel situation can be recovered to some extent. This is the information that is used by precoding algorithms to make decision on precoder selection.

G-RAKE extension in MIMO

In a 2×2 MIMO system, the effective channel coefficient matrix can be rewritten as $\hat{\mathbf{H}}_{\text{eff}} = [\hat{\mathbf{h}}_{\text{eff1}} \quad \hat{\mathbf{h}}_{\text{eff2}}]$, where $\hat{\mathbf{h}}_{\text{eff1}}$ and $\hat{\mathbf{h}}_{\text{eff2}}$ are column vectors that contain the channel estimation values for each stream. Recall the G-Rake combining weight function in eq. (2.22), the associated G-Rake combining weight w_1 and w_2, which represented data stream 1 and 2, satisfying

$$(\mathbf{R}_u + \hat{\mathbf{h}}_{\text{eff2}}\hat{\mathbf{h}}_{\text{eff2}}^H)\mathbf{g}_1 = \hat{\mathbf{h}}_{\text{eff1}} \tag{2.49}$$

and

$$(\mathbf{R}_u + \hat{\mathbf{h}}_{\text{eff1}}\hat{\mathbf{h}}_{\text{eff1}}^H)\mathbf{g}_2 = \hat{\mathbf{h}}_{\text{eff2}}, \tag{2.50}$$

This equation set is the MIMO extension of G-Rake combining weight calculation [24].

Limited feedback

In a communication system, feedback can be used to enable the transmitter to exploit the channel conditions and thus avoid interference. For MIMO networks, with channel information known at the transmitter (which is called closed-loop MIMO communication [13]), the transmitted waveforms can be customized to gain higher link capacity and throughput. However, as it has been stated in the problem of precoding in MIMO systems in chapter 1, it is not efficient to have full channel information at the transmitter since the cost of overhead information is far larger than the benefit from the improvement of link throughput in real systems. In this case, limited feedback communication is one promising solution to this problem.

The basic idea lying behind is to utilize vector quantization techniques to quantize channel state information over a limited data rate feedback channel [13]. The aim of

limited feedback is not to reconstruct the channel of interest completely, but to make a good vector quantization approach that would obtain a good approximation on the channel realization.

Normally, the precoder is a complex matrix, $\mathbf{W}$. The number of rows of the precoder matrix corresponds to the number of antenna ports, and the number of columns corresponds to the number of streams. According to the standard of 3GPP specifications of release 7 and 8 [25], in 2×2 MIMO, there are four precoders provided to select from. One solution is

$$\mathbf{W} \in \left\{ \frac{1}{\sqrt{2}} \begin{bmatrix} 1 & 1 \\ 1 & -1 \end{bmatrix}, \frac{1}{2} \begin{bmatrix} 1-j & 1-j \\ 1+j & -1-j \end{bmatrix}, \frac{1}{\sqrt{2}} \begin{bmatrix} -j & -j \\ j & -j \end{bmatrix}, \frac{1}{2} \begin{bmatrix} -1-j & -1-j \\ -1+j & 1-j \end{bmatrix} \right\}. \tag{2.51}$$

There are four precoding weights in a precoder. It can be observed that

$$w_{21} = w_{11}, w_{12} = w_{11}^*, w_{22} = -w_{12}. \tag{2.52}$$

The first stream is multiplied with w_{11} and w_{12}, and the second stream is multiplied with w_{21} and w_{22}. w_{12} is selected by the base station and transmitted as the feedback, then w_{11}, w_{21} and w_{22} can be derived from w_{12} by the UE. The base station selects the optimum weight factors based on proposals reported by the UE in the uplink.

It can be seen that in all precoders, the first column vector and the second column vector are orthogonal, that is

$$\begin{bmatrix} w_{11} \\ w_{12} \end{bmatrix}^H \begin{bmatrix} w_{21} \\ w_{22} \end{bmatrix} = 0. \tag{2.53}$$

This is an essential property of a precoder in the limited feedback condition. It ensures that the two streams are kept orthogonal after precoding. Hence, no extra interference will be introduced by the precoding process.

The phase difference between the two elements of each column in the precoding matrices ($\phi_{12} - \phi_{11}$ and $\phi_{22} - \phi_{21}$, where ϕ_{xy} stands for the phase angle of precoding element w_{xy}) is a key issue in designing precoders, since it controls how the beamforming for the two streams works. In the case of four precoders shown in eq. (2.51), the phase differences of the two elements in the first column are 0, $\pi/2$, π and $3\pi/2$, respectively.

To further explain the phase property of a precoder, let us consider a precoding procedure as an example. Denoting the signal on the transmitter antennas as $\tilde{s}_1(t)$ and $\tilde{s}_2(t)$, we have

$$\begin{aligned} \tilde{s}_1(t) &= w_{11}s_1(t) + w_{21}s_2(t) \\ \tilde{s}_2(t) &= w_{12}s_1(t) + w_{22}s_2(t). \end{aligned} \tag{2.54}$$

For the signal received by the first receiver antenna $r_1(t)$, it will be a mix of $\tilde{s}_1(t)$ and $\tilde{s}_2(t)$, i.e.,

$$r_1(t) = h_{11}(t)\tilde{s}_1(t) + h_{21}(t)\tilde{s}_2(t). \tag{2.55}$$

As a 2×2 precoding aims at forming two parallel channels, we assume that the first receiver antenna is for receiving the primary stream $s_1(t)$, and rewrite the equation as

$$\begin{aligned} r_1(t) &= h_{11}(t)[w_{11}s_1(t) + w_{21}s_2(t)] + h_{21}(t)[w_{12}s_1(t) + w_{22}s_2(t)] \\ &= [h_{11}(t)w_{11} + h_{21}(t)w_{12}]s_1(t) + [h_{11}(t)w_{21} + h_{21}(t)w_{22}]s_2(t). \end{aligned} \tag{2.56}$$

Suppose no phase difference is introduced by $h_{11}(t)$ and $h_{21}(t)$, or in other words, the phases of $h_{11}(t)$ and $h_{21}(t)$ are the same, in order to maximize the power of $s_1(t)$, the phase of w_{11} and w_{12} should be identical, i.e.,

$$\phi_{11} = \phi_{12}. \tag{2.57}$$

In the codebook shown by eq. (2.51), the first precoder fulfills this condition. Then look into the relation between the elements in the second column of this precoder, the phase difference $\phi_{21} - \phi_{22}$ is π. Hence, the remaining term for the secondary stream in eq. (2.56) (i.e., $[h_{11}(t)w_{21} + h_{21}(t)w_{22}]s_2(t)$) is minimized on this receiver antenna.

The idea of precoding in limited feedback condition is to choose the most suitable precoder from the codebook based on the channel information. According to the derivation above, phase difference turned out to be a very significant characteristic. For a desired stream, if the phase difference of the corresponding precoding weights is equal to the phase difference between the channels, this stream can be maximally received and the other stream can be thus maximally suppressed at the same time. Hence, the crosstalk is maximumly mitigated. As a consequence, the phase property of a precoder could be one clue for making a good choice. This derivation is also considered as a motivation of the algorithms discussed in chapter 4.

3

WCDMA standardization and simulator description

This chapter describes the fundamentals of our simulation. WCDMA standardization is briefly introduced firstly as a motivation of the simulator structure and parameter selection. This is followed by the simulator description, which starts with several assumptions we made. The simulator is split into parts and all functions are explained, where all results carried out in chapter 4 are based on it.

3.1 WCDMA standardization

WCDMA is an air interface standard that is generally used in 3G networks. It was firstly developed in the late 1990s, and accepted by International Telecommunication Union (ITU) as a portion of the International Mobile Telecommunications for the year 2000 (IMT-2000) before it became a standard of Universal Mobile Telecommunications System (UMTS). WCDMA implements the DS-CDMA technique on a pair of channels with a fixed bandwidth of 5MHz, which is four times wider than the 1.25MHz bandwidth used by another 3G standard CDMA2000. With a lot of advantages like the flexibility in providing different types of service, WCDMA was selected for the evolution from 2G GSM towards 3G, and gain a large part of the 3G market share [3, 10].

3GPP, also known as the organizational partners, is the global standards-developing organization that has been standardizing WCDMA since the end of 1998. It involves six organizational partners (ARIB, CCSA, ETSI, ATIS, TTA and TTC). Several elements of the WCDMA standard that are essential for this thesis are described below.

3.1.1 Physical layer channels

For a regular WCDMA UL SISO transmission, the control information of physical layer is included in a Dedicated Physical Control Channel (DPCCH). Higher layer information including user data is in the Dedicated Physical Data Channel (DPDCH). DPCCH is mapped to the in-phase branch of an M-ary Quadrature Amplitude Modulation (M-QAM) modulation, while the corresponding DPDCH is mapped to the quadrature branch [3].

Enhanced uplink uses Enhanced Dedicated Physical Data Channel (E-DPDCH) instead of DPDCH to increase the throughput. In this context, an additional channel, Enhanced Dedicated Physical Control Channel (E-DPCCH), is used for extra control information transmission [26]. This enhanced uplink is implemented for MIMO. In MIMO transmission, Secondary Dedicated Physical Control Channel (S-DPCCH) and Secondary Enhanced Dedicated Physical Data Channel (S-E-DPDCH) are implemented on the secondary stream. The control information for S-E-DPDCH is included in Secondary Enhanced Dedicated Physical Control Channel (S-E-DPCCH) that is allocated on the primary stream. Both E-DPDCH and S-E-DPDCH are using I and Q branches. E-DPCCH is always mapped to the I branch and S-E-DPCCH is always mapped to the Q branch of the primary stream. The DPCCH and S-DPCCH are always mapped to the Q branch [26]. MIMO physical channel allocation is shown in figure 3.1.

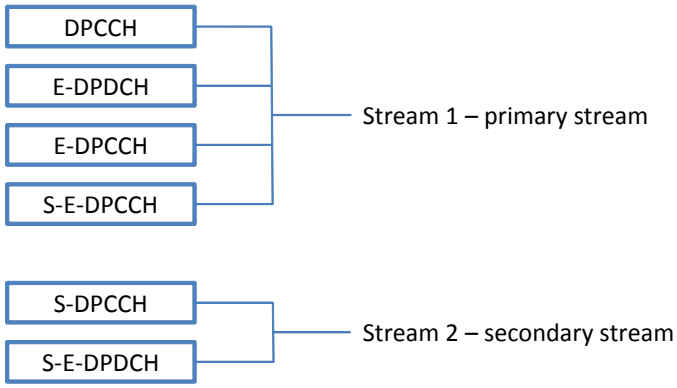

Figure 3.1: Channel allocation of MIMO.

3.1.2 Frame structure

An uplink frame has a duration of 10 ms. Each frame contains 15 slots, while each slot has a length of 2560 chips, corresponding to a duration of 666 μs. Within each slot, DPCCH contains four parts: pilot, Transport Format Combination Indicator (TFCI), Feedback Information (FBI) and Transmission Power Control (TPC). A single-code DPDCH transmission is beneficial from making amplifiers more efficiently, but for higher data rate requirement, multicode transmission is implemented, leading to a maximum data rate of 2 Mbps [3].

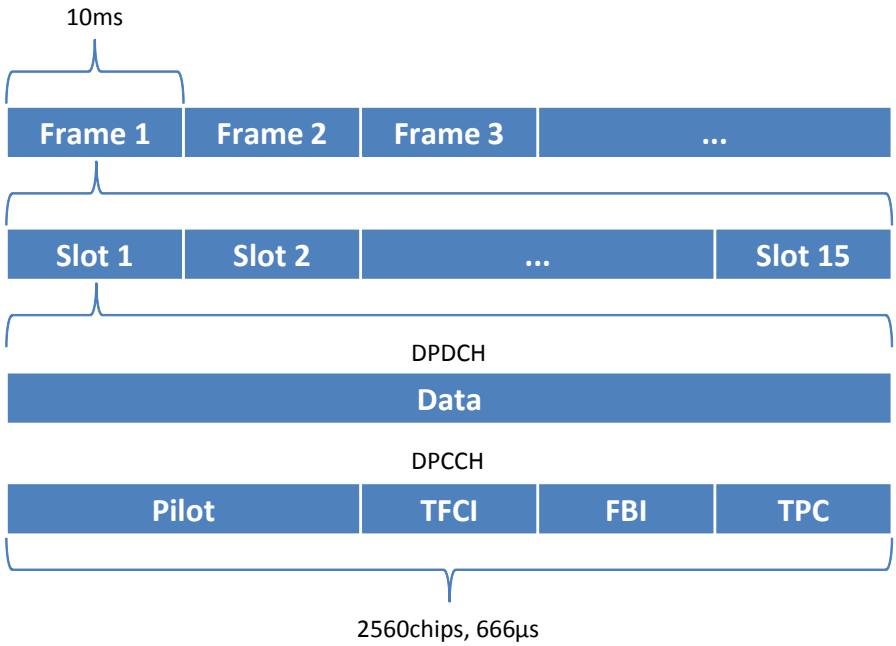

Figure 3.2: WCDMA uplink frame structure. Each frame contains 15 slots, where each slot contains DPDCH and DPCCH.

3.1.3 Channel coding and interleaving

To enhance data reliability, channel coding is implemented. It is done by adding additional bits to protect the information bits from the noise and interference. Currently there exists a number of coding methods, e.g., repetition coding, block coding and convolutional coding [22]. Denoting the data bit sequence with length K as $\mathbf{u}^K$, the coded bit sequence after channel encoder with length N as $\mathbf{c}^N$, then the ratio K/N is called coding rate, which shows the redundancy added by channel coding. In the standard, turbo coding is used for data service.

Interleaving further increase the robustness of the transmission reliability by separating coded bits with a random interval. By doing this, the probability of losing adjacent coded bits decreases, giving out a larger chance to recover the data bits successfully [3].

3.1.4 Spreading and scrambling

Spreading is used to spread the user signal into a wider frequency band using spreading codes. In WCDMA uplink, the SF has a fixed value of 256 for the DPCCH, which is the highest possible value in the standard. The DPDCH has an SF range from 4 to 256 [3]. An additional SF option is 2,2,4,4 for E-DPDCH, i.e., one pair of branches with SF $= 2$ using M-QAM, and there is another pair of branches with SF $= 4$ on the top of it. The two pairs of spreading codes must be orthogonal.

Scrambling is on the top of spreading. This process is used for separating different

terminals or base stations. Different scrambling codes are used on top of channelization code trees, so that identical codes can be used for spreading by different terminals. Synchronization must be obtained by the descrambling to perform a successful decoding. Hence, the orthogonality of the channelization codes can be reserved [3].

3.1.5 Power control

WCDMA system is based upon power control. Considering that one UE is suffering a bad transmission condition, e.g., deep fading, in order to deal with this matter, the UE will increase its transmission power until it is satisfied with the link quality. Since WCDMA users share the same bandwidth, this overpowered UE hence becomes a huge interference source for the other UEs, and thereby block a large part of the cell [3]. There are two main techniques for solving this problem: open-loop power control and closed-loop power control.

Open-loop power control roughly estimates the path loss, and gives a UE a power setting according to the estimation results. This method is inaccurate and slow, focusing on providing an initial setting, thus closed-loop power control can work based on it.

A fast closed-loop power control method is used to further compensate for the fast-fading channel. SINR is frequently estimated at a base station and comparison with a target SINR is made. If the estimated value is smaller than the target, the UE will be required to increase its power; if the estimated value is larger than the target, the UE will be required to decrease the power. As this mechanism performs in a fast way, the fast fading can be compensated without overpowering a UE [3].

3.1.6 WCDMA channel model

The ITU channel model Pedestrian A (PA) is chosen as the primary model for testing, which is defined in 3GPP TR 30.03U [27]. The taps of a Pedestrian channel are Rayleigh fading with flat Doppler in the case of no LOS component. The multipath intensity profile of the PA is defined as follows:

Relative Delay(ns)	0	110	190	410
Relative Power(dB)	0.0	-9.7	-19.2	-22.8

3.2 Simulator overview and assumptions

This section describes the WCDMA UL simulation environment, which is built using IT++. An overview of the entire simulator structure is introduced, followed by all assumptions we made. Functionality is specified in the next sections block by block.

The simulator contains a simplified WCDMA transmission link. Some main parameters in our simulator follow the 3GPP standard. Both MIMO and SISO models can be selected, while AWGN and TDL channel models are available for testing.

Transmission starts with physical channel generation. Both data channels and control channels are generated at this stage. These physical channels will be spread, split into

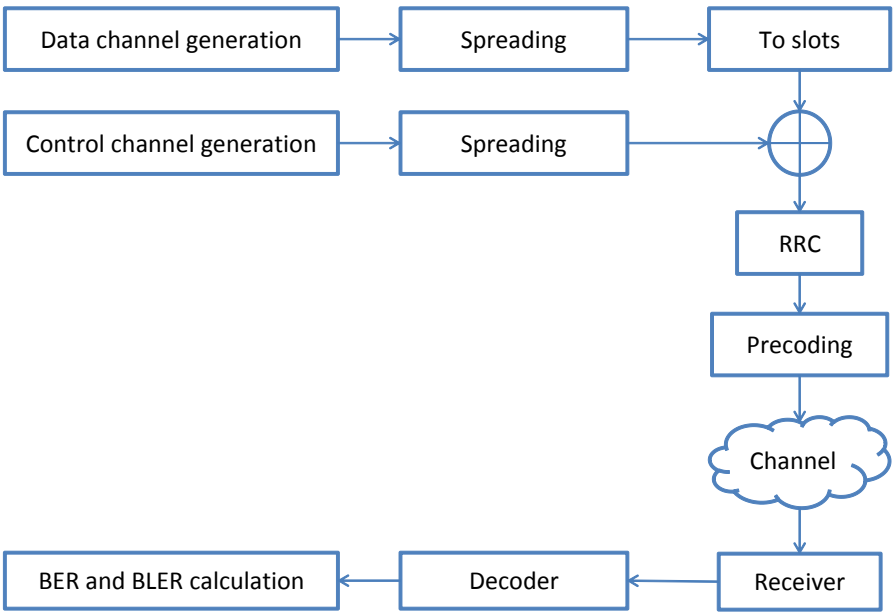

Figure 3.3: Simulator structure.

slots and merged. Each slot will be pulse shaped, and precoded if MIMO model is selected, before sending over the transmission channel. The signal passed through the channel will be collected by a receiver and sent to a decoder module. The decoded data bits are used for BER and BLER calculation. See figure 3.3.

For simplification of the simulator, power control is not implemented in our simulator though it is an essential element in the WCDMA standard. In the standard, Hybrid Automatic Repeat Request (HARQ) retransmission will be applied to reduce BLER [26]. In our simulator, retransmission is not implemented either, since it will not affect the comparison results of precoding algorithms.

Several assumptions are made in our simulation process.

- Transmission is continuous.
- Signals are only transmitted in the base-band, i.e., signals are not modulated up to any carrier frequency.
- The channel has slow fading.
- The distance between the transmitter and receiver is far larger than the distance of the two receive antennas, so that the two antennas receive the signals at the same time can be assumed.
- The distance between the two receive antennas is larger than half of the wavelength of the carrier, so that the channels seen by the receive antennas to be independent can be assumed.

- The channel input and the output signal power are the same, i.e., perfect power control is assumed.

3.3 Simulator specification

3.3.1 Data channel generator

This block generates the data channels and control channels for a frame, giving out a certain number of symbols. For DPDCH generation, the number of output symbols is 9600, while for E-DPDCH generation, the number of output symbols is 57600, corresponding to an entire frame. The procedure inside this block includes four steps: data bit generation, turbo encoding, interleaving and modulation.

Data generator

Random bits are generated as data bits. 3196 bits are generated every time this block is called, making a DPDCH frame. For E-DPDCH generation, six times longer bits (the same as six standard frames) will be created each time since E-DPDCH sends six times longer data at the same time with a more complex mapping.

Turbo coding

Turbo coding is used for data coding to reduce errors on the data channels. The generator polynomials are chosen as "013" and "015". The constraint length of the two constituent encoders was chosen as 4. The number of iteration was 8. The interleaving sequence we used was WCDMA turbo interleaver sequence with 3196 bits, which is generated as the internal turbo encoder interleaver for WCDMA [14]. The algorithm used to decode turbo codes is "LOGMAX", which is a simplification of the Maximum a Posteriori (MAP) based decoding algorithm.

Interleaving

After turbo coding, the coded data is further processed by interleaving. Block interleaving with 4×4 matrix is applied.

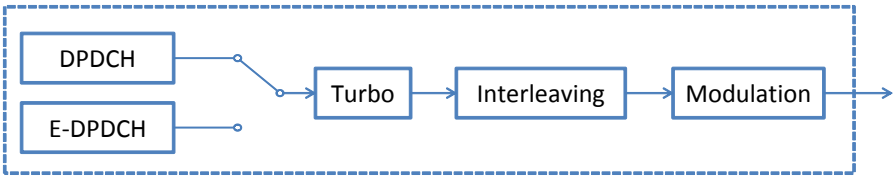

Figure 3.4: Data channel generator structure. Two kinds of data channel can be generated. Data bits are encoded by a Turbo encoder and then interleaved by a block interleaver. Afterwards, bits will be modulated into symbols and sent to the spreading block shown in the figure 3.3.

Modulation

BPSK is used for data channel modulation. Thus, for E-DPDCH generation, four data symbol sequences with a total number of 57600 bits will be the output. These sequences will be merged into one afterwards.

3.3.2 Control channel generator

As the only usage of DPCCH is channel estimation, 10 bits are generated as a pilot. The pilots are assumed to be known at the receiver, so no channel coding will be used for control channel.

3.3.3 Spreading

For DPDCH, spreading factor SF = 4 is used. The output will be a chip sequence with length equal to 38400. For E-DPDCH, spreading factors SF = 2,2,4,4 is used, resulting into four sequences with 38400 chips in each sequence. Those sequences are mapped on I and Q branches separately, i.e. one SF = 2 sequence and one SF = 4 sequence are mapped on branch I, and the other two sequences are mapped on branch Q. For DPCCH, spreading factor SF = 256 is used. Since the higher the spreading factor is, the larger spreading gain will be achieved as mentioned in chapter 2, so SF = 256 gives better protection on the pilot bits. The output sequence length then is 2560.

3.3.4 Slot-wise transmission

According to the standard [3], a frame contains 15 slots, and each slot contains 2560 chips. Hence, a data channel sequence that contains 38400 chips, will be split into 15 slots equally.

As the transmission is assumed to be continuous, i.e., no gap between two frames, at the beginning and the end of a slot the receiver should be able to see interference from the adjacent slots. Thus, each slot will have 20 chips from the previous and the next slot attached, resulting in a "slot" length of 2600 instead of the standard length of 2560 as shown in figure 3.5. Channel estimation should be able to be performed based on slot. Thus, DPCCH is attached to each slot, which also contains extra DPCCH chips from adjacent slots as described for DPDCH.

For the first slot, since no earlier slot can be seen, half of the extra chips are taken from the end of this frame. Similarly, the last slot copies 20 chips from the head of this frame.

3.3.5 RRC pulse shaping

RRC pulse with a roll-off factor RF = 0.22 is used for pulse shaping, as standardized [3]. Filter length is selected as six and up-sampling rate is selected as eight.

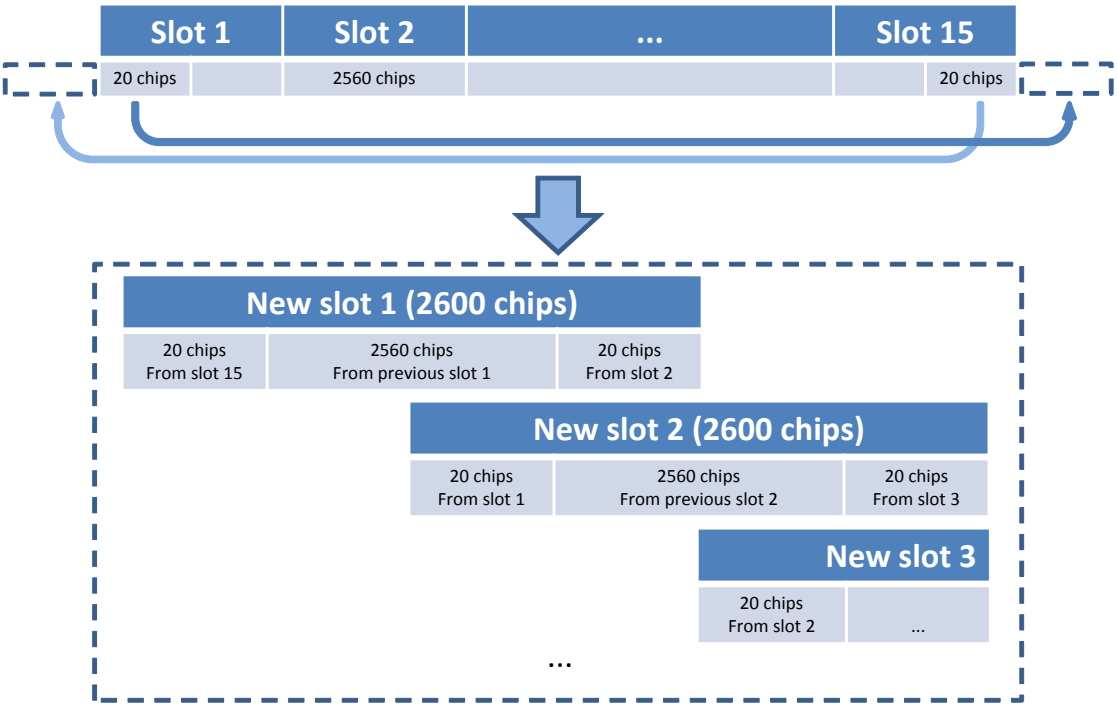

Figure 3.5: Slot-wise transmission. Each slot will be padded 10 chips from the previous and the next slot, forming a new transmission slot with 2600 chips in order to simulate the continuous transmission. The first slot will get half of the extra bits from the 15th slot and the 15th slot will get half from the first slot as well.

3.3.6 Precoding

This block takes the previous estimation matrix and RRC output samples as input and gives coded sequences as output. Precoding matrix is decided by the algorithm selection. Both unlimited and limited feedback precoding can be simulated.

The basic mechanism of precoding is shown in figure 2.7. Two kinds of precoding methods are tested in our simulator: unlimited feedback and limited feedback. In the case of unlimited feedback, full channel information can be sent to the transmitter from the receiver to decide the precoder that will be used. In the case of limited feedback, only precoding index will be sent from the receiver to tell the transmitter which precoding matrix should be used.

3.3.7 Channel model

Single line transmission

Three channels were implemented and tested in the beginning with SISO simulation shown in figure 3.6, AWGN channel, generic TDL channel and PA channel. In AWGN channel, noise variance range was set from -6 dB to 32 dB. In TDL channel, we used 2

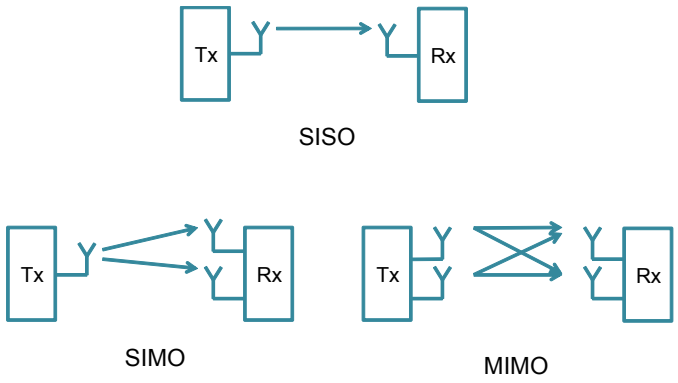

Figure 3.6: Channel models. Three channels models are tested in our simulator: SISO, SIMO and MIMO.

taps with different power profile and delay profile. The sampling time was set to 32.55×10^{-9} s which was the standard chip time 260.4×10^{-9} s divided by the upsampling rate. In PA channel, since it is a special case of TDL channel, the IT++ defined TDL function is called to generate the PA channel with channel specification to be *ITU_Pedestrian_A*. The doppler is set to be a very small number (10^{-28} s) so that each frame will see a flat fading channel. Deep fading characteristic was simulated by setting a new channel realization for every frame (see Simulator evaluation).

Diversity channel model

This so-called "diversity channel model" is defined for simulating receiver spatial diversity, referring to the SIMO model. In this model, one transmitter antenna will send signal to two receiver antennas through independent channels. Same channel types are used as with the SISO model. For two transmission data streams the simulator forms two parallel SIMO systems, which gives spatial diversity gain.

MIMO channel model

For MIMO system, crosstalk is introduced in the channel model. Four channel realizations are generated for each frame. Thus, for a single transmission, there will be two data streams that are passing through two independent channels and arrive at each receiver antenna simultaneously. According to the assumptions, the two streams will be added up at the receiver antennas before passing through the matched filter.

3.3.8 Receiver

Matched filter and down-sampling

Same RRC as used in pulse shaping is employed as the matched filter. Since the effect of the convolution operation, i.e., every convolution will increase the sequence length by

Figure 3.7: The picture shows the preamble we used in the simulation. One extra slot with only DPCCH is added before each frame to achieve "ideal" channel estimation.

the filter length, the length of the filtered sequence is increased. As the sequence has been passed through the pulse shape filter and the matched filter, the down-sampling process will ignore the number of filter length samples on both ends, and pick every one out of eight samples with a correct timing.

RAKE and G-RAKE receiver

The structure of the Rake receiver is shown in the figure 2.5. For Rake, the number of fingers is the same as the number of taps of the channel. For G-Rake, since we are using a PA channel, which has four taps, the number of fingers is chosen to be 5. The core principle for finger placement is that the fingers need to cover all the taps in the channel, even if they are not perfectly matched with the taps. In the simulations, Rake and two G-Rake receivers (with CS term and without CS term) were tested to see the influence of equalization to the performance of precoding.

Channel estimation

In our simulator, channel estimation is utilized in two parts. One is in the G-Rake receiver. The other is before transmission, which is to estimate the effective channel in order to calculate the precoding matrix (see eq. (2.47)). DPCCH and S-DPCCH are used for channel estimation. The channels are estimated using the pilots in the control channels. A spreading sequence with a SF of 256 is applied for the control channel.

Channel estimation is essential in order to calculate corresponding combining weight for each finger in the G-Rake receiver. In MRC, the channel fading and phase rotation caused by reflection, dispersion, etc., are compensated by multiplying the received signal by the conjugation of the estimated channel. In this case, the channels are different observed by different fingers in the G-Rake receiver.

For the estimation of the effective channel, we aim to estimate the precoded effective channel on each tap. This estimated effective channel is our key basement for deciding the precoding index we used for precoding. In our simulation scenario, a preamble that contains a slot of control channel will be sent before the transmission of each frame, in order to calculate the precoder for the first slot. In the appendix section "Channel estimation error", the normal slot-based estimation and preamble-based estimation are evaluated and compared.

Figure 3.8: The structure of decoder is shown in the picture. Received slots will be reshaped and de-interleaved, and then send to Turbo decoder. Decision is made inside Turbo decoder, and decoded data bits are sent as output.

3.3.9 Decoder

Slot-wise reshaping

The structure of the decoder is shown in figure 3.8. In order to decode the data bits, slots will be reshaped back into a frame. Extra chips are discarded during MRC if G-Rake is used, or during despreading if a simple receiver is used.

De-interleaving, Turbo decoding and decision

These are inverse processes of data channel generation. Soft bits are de-interleaved and sent to the Turbo decoder. Decision is made by the Turbo decoder as well.

3.3.10 BER and BLER calculation

BER is measured on data bits. Both streams are evaluated separately and total BER is measured as well. BLER is measured instead of real throughput. A frame is defined as a block, hence, a frame with non-zero BER is defined as a block error. Each SNR would give a BER and a BLER value.

4

Algorithms and results

In this chapter, several algorithms are introduced and the simulation results are presented. First of all, the simulations of the SVD algorithm with CS term and without CS term in the equalization are implemented. Then Closest-to-SVD (CSVD) algorithms based on SVD in the case of limited feedback are tested when using distance and phase separately for judging and the results are shown. At last, the results of the CSVD algorithm using preamble-based channel estimation (referred to as preamble-based CSVD) is presented.

4.1 Two ways of mitigating crosstalk in MIMO

According to [10], there are two ways to decrease the impact of MIMO multiplexing crosstalk: equalization and precoding. Precoding aims at separating the streams, so that the crosstalk interference can be minimized at the transmitter side, and equalization aims at further suppressing or canceling the crosstalk interference at the receiver side. In this section, the G-Rake receiver based MMSE equalization method is applied and the performance with CS term and without CS will be compared.

4.1.1 Special interference suppression term in MIMO equalization

In WCDMA, the equalization happens in the RAKE receiver. Recall the combining weight eq. (2.22), it can be reconstructed as

$$\mathbf{R}_u \mathbf{g} = \hat{\mathbf{h}}. \tag{4.1}$$

For convenience, let us bring equations 2.49 and 2.50 here:

$$\begin{aligned} (\mathbf{R}_u + \hat{\mathbf{h}}_2 \hat{\mathbf{h}}_2^H)\mathbf{g}_1 &= \hat{\mathbf{h}}_1, \\ (\mathbf{R}_u + \hat{\mathbf{h}}_1 \hat{\mathbf{h}}_1^H)\mathbf{g}_2 &= \hat{\mathbf{h}}_2, \end{aligned} \tag{4.2}$$

where $\hat{h}_k$ stands for the effective channel (according to eq. (2.47)) of stream k. Comparing with the 2×2 MIMO extended equations 4.2, there is an extra term $\hat{h}_k \hat{h}_k^H$. This term works on suppressing the interference (from stream k) [24], i.e., CS. For instance, k will be 2 for stream 1 and vice-versa.

4.2 Simulation configuration

In our simulator, 4000 frames are ran for each simulation in order to get a reasonable statistics and a smooth curve. Both BER and BLER are calculated and performance of BLER is shown in the figures for comparison. SNR is defined as E_b/N_0 in the receiver side. In all the simulations, fixed precoding index method is used as a benchmark. This is done by firstly randomly choosing one precoder from the four available precoders and then the selected one is used for precoding in all frames. For instance, if the second precoder is chosen, all frames will use the second precoder for precoding.

For the BLER comparison, mainly the performance in the low SNR range (from 2 dB to 10 dB) will be discussed. One reason why only relatively low SNR range is discussed is that for an uplink, the transmit power in the UE side should not be too high in order to keep power consumption low. Another reason is that in a real multi-user WCDMA system, one single user could not maintain power in a very high level, otherwise, the other users will suffer from high interference and need to increase its power as well to keep normal transmission, which as a result will make power control unmanageable.

4.3 Unlimited feedback

4.3.1 Without the CS term

We first consider the SVD method without CS (eq. (4.1)). The total BLER curves are shown in figure 4.1(a) and the stream-wise BLER curves are shown in figure 4.1(b), respectively for the result of SVD algorithm, fixed precoding and no precoding. From the figure 4.1(a), the SVD precoding curve shows an obvious gain in terms of total BLER. It has a positive effect on minimizing the crosstalk interference even in frequency selective channel.

In addition, while SNR exceeds 18 dB, the BLER curve reaches an error floor. One possible reason is that after reaching some SNR value, the remaining interference dominates the system performance. As a result, keeping increasing power will not help. Equalization must be employed to mitigate the remaining interference in order to get a good result. Since the floor of BLER is around 0.65, which is much higher than acceptable, using precoding alone to deal with the crosstalk turns out to be not enough.

Looking at the figure 4.1(b), we can see that there is a difference between streams with the SVD method. The BLER of the primary stream goes down to 0.3, while the secondary stream suffers from a BLER value very close to 1 no matter how high the SNR increases. By implementing the SVD method, the system gain a relatively better performance with the cost of secondary stream. This will lead to a practical problem

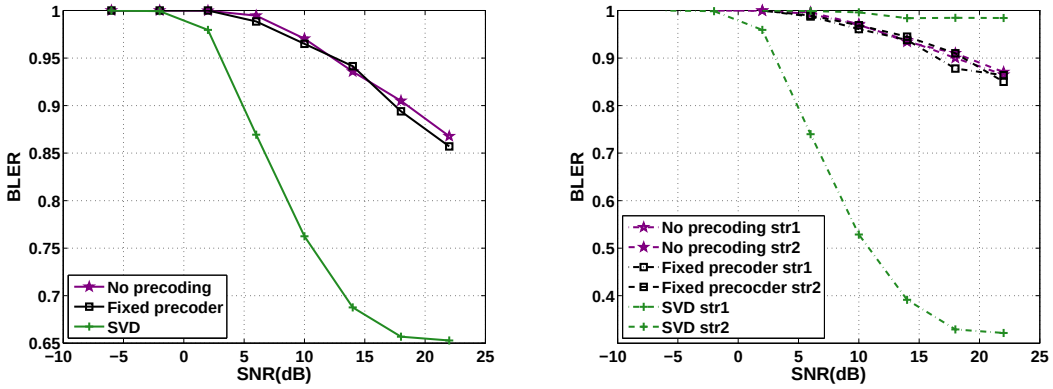

(a) Total BLER

(b) Stream BLER

Figure 4.1: These are the resulted BLER curves without CS in unlimited feedback case. Left one shows that SVD gives an obvious gain in terms of total BLER, while the right one shows the difference of performance between the two streams of SVD. See legend explanation in section 4.6 Explanation of the legends.

that the primary stream gains a relatively high throughput but the throughput of the secondary stream is nearly zero.

4.3.2 With the CS term

With CS (eq. 4.2), the performance becomes much better (see figure 4.2(a) and 4.2(b)). Total BLER values are going down to 0.12 while increasing SNR. There is a considerable gain from SVD (0.6 dB at BLER equal to 0.5) comparing with the fixed precoding index method. Both SVD and fixed precoding gives a higher error floor value than the curve without precoding.

In figure 4.2(b), we can see that the difference in performance between the two streams is similar to that observed in figure 4.1(b), which mainly results from the characteristic of SVD where the singular value of the primary stream is always larger (see eq. 2.40).

As standardized, the primary stream contains most of the control information (i.e., DPCCH, E-DPCCH and S-E-DPCCH). By making the primary stream robust, this information will benefit from a higher SNR and has a better chance to be decoded successfully. With more reliable control channels, the SVD method can further improve the system even though the total BLER have not shown essential gain.

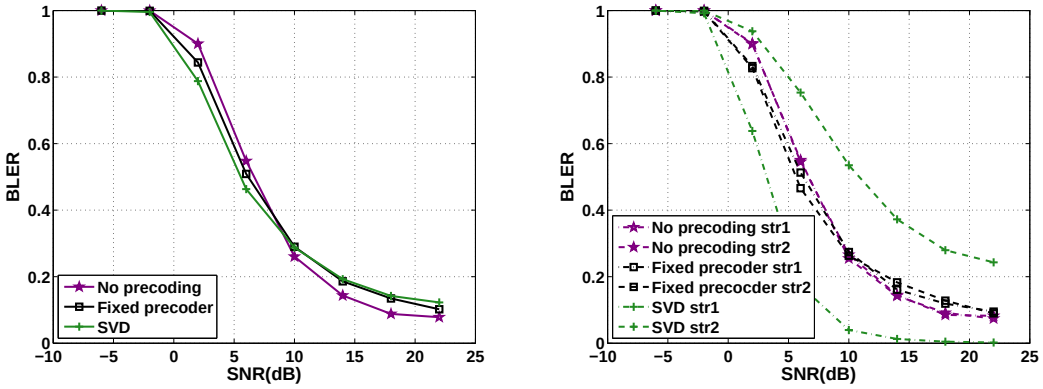

(a) Total BLER

(b) Stream BLER

Figure 4.2: These are the BLER curves with CS in unlimited feedback case. BLER of SVD is lower than the one with fixed precoding when SNR is -6 dB to 10 dB with a BLER gain of 0.6 dB. After 10 dB SNR, the BLER of SVD is higher than the one with fixed precoding. The primary stream BLER goes towards zero when SNR increases. See legend explanation in section 4.6 Explanation of the legends.

4.4 Limited feedback

4.4.1 Upper bound and lower bound

In order to calculate the gain achieved by choosing the precoder that gives the best BER performance for every frame, we simulated all four precoders from a pre-defined codebook for each channel realization. BER was calculated frame-wise, and the best and the worst performance for each channel realization was recorded. Fixed precoding result is also included as a reference for comparison. The best precoder ($\mathbf{W}_\mathrm{b}$) is selected by,

$$\mathbf{W}_\mathrm{b} = \arg\min_{\mathbf{W}^k} \mathrm{BLER}, \mathbf{W}^k \in P \tag{4.3}$$

and similarly, the worst precoder ($\mathbf{W}_\mathrm{w}$) is selected by,

$$\mathbf{W}_\mathrm{w} = \arg\max_{\mathbf{W}^k} \mathrm{BLER}, \mathbf{W}^k \in P \tag{4.4}$$

where BLER is the total BLER of each frame in simulation and $\mathbf{W}^k$ is one of the four precoders. Recalling the eq.(2.51), we denote the set of the four precoders as P and $\mathbf{W}^k$ belongs to one of the precoders ($\mathbf{W}^k \in P$), i.e.,

$$P = \left\{ \frac{1}{\sqrt{2}}\begin{bmatrix} 1 & 1 \\ 1 & -1 \end{bmatrix}, \frac{1}{2}\begin{bmatrix} 1-j & 1-j \\ 1+j & -1-j \end{bmatrix}, \frac{1}{\sqrt{2}}\begin{bmatrix} -j & -j \\ j & -j \end{bmatrix}, \frac{1}{2}\begin{bmatrix} -1-j & -1-j \\ -1+j & 1-j \end{bmatrix} \right\}. \tag{4.5}$$

It can be seen from the results shown in figure 4.3 that, for four precoders, there is an obvious difference (about 3 dB in average) between choosing the best precoder and

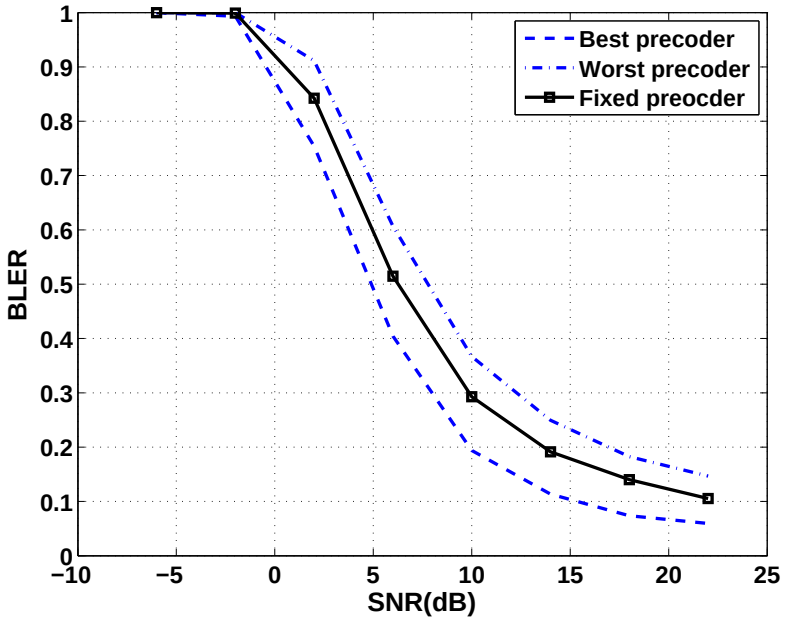

Figure 4.3: This figure shows a comparison of performance of best, worst and fixed precoders in the case of limited feedback. There is about 3 dB gain between the best precoder and the worst precoder in limited feedback case. The gain between best precoder and fixed precoder is about 1.2 dB at BLER of 0.5. See legend explanation in section 4.6 Explanation of the legends.

the worst precoder, and the gain between best precoder and fixed precoder is around 1.2 dB at BLER of 0.5. That means, with the current system the maximum achievable gain is 1.2 dB, if the best precoder is used.

4.4.2 Two approaches of implementing SVD algorithm with limited feedback

As mentioned before, the SVD algorithm has shown some gain comparing with the fixed precoding method. Hence, it is meaningful to find a suitable approach to implement this algorithm when only limited feedback is available at the UE side. Recalling the eq. (2.35), we tried to select the precoder that is closest to some characteristics of the SVD resulted precoding matrix $\mathbf{V}$: either from the distance, or from the phase. In this thesis, this method is referred to as CSVD algorithm.

Judged by distance

The first approach we tested was to calculate the distance between one of the available precoders $\mathbf{W}^k$ and the $\mathbf{V}$ returned by SVD. Denoting the minimum distance as D, then

the precoder we choose ($\mathbf{W}^d$) based on distance is expressed as,

$$\mathbf{W}^d = \arg\min_{\mathbf{W}^k} D = \arg\min_{\mathbf{W}^k} \sum_{i=1}^{2}\sum_{j=1}^{2}(w_{ij} - v_{ij})^2, \mathbf{W}^k \in P \tag{4.6}$$

where i, j represents the row and the column in the matrix $\mathbf{W}^k$ and $\mathbf{V}$. Comparing with the method of fixed precoder, the algorithm of CSVD judged by distance shows no gain, as shown in figure 4.4.

Judged by phase

Recalling the section 2.2.2 in chapter 2, phase is a vital feature for precoding matrices. The phase difference of the two elements of each column in the precoder matrix represents the way of beamforming for each streams. Then we calculate the phase difference of first column in $\mathbf{V}$, and choose the precoder that has the closest phase difference with $\mathbf{V}$. Denoting the phase distance between a standardized precoder and $\mathbf{V}$ as D_{phase}, the precoder we choose ($\mathbf{W}^p$) based on phase is expressed as,

$$\mathbf{W}^p = \arg\min_{\mathbf{W}^k} D_{\text{phase}} = \arg\min_{\mathbf{W}^k} |(\phi(w_{12}) - \phi(w_{11})) - (\phi(v_{12}) - \phi(v_{11}))|, \mathbf{W}^k \in P \tag{4.7}$$

where w_{ij} and v_{ij} represent the element of jth row and ith column in matrix $\mathbf{W}^k$ and $\mathbf{V}$ respectively and $\phi(\cdot)$ is the phase of a complex value. As shown in figure 4.4, this phase-based algorithm of CSVD shows a gain of 0.4 dB compared to fixed precoder method in relatively low SNR range (from 2 dB to 10 dB). However, no improvement on the error floor can be seen.

4.4.3 Preamble-based CSVD

Since the normal channel estimation is slot-based as mentioned in chapter 3, and the decision of selecting precoder is based on the channel estimation from the previous slot, we always observe a channel estimation error. The most likely reason, as we investigated, is that the evaluation of interference from the previous slot is no longer suitable for the current slot (see appendix section “Channel estimation error”). To achieve more reliable estimation, we tested the algorithm with frame-based channel estimation, that only preamble for channel estimation as mentioned in section 3.3.8. In this case, a slot that contains only pilots will be added before each transmitted frame to estimate the channel and no control channel will be used. With frame based channel estimation, the preamble of every frame is used for the channel estimation for a whole frame (15 slots).

It can be seen from the figures 4.4 and 4.5 that the performance of the preamble-based CSVD algorithm is better than the fixed precoder with a gain of about 0.6 dB in relatively low SNR range. Moreover, performance of the primary stream is always much better than that of the secondary stream in this case (about 1 dB difference), which is similar to the behavior as the SVD in unlimited feedback conditions. After SNR exceeds

18 dB, the curve reaches an error floor which is nearly the same as the one with fixed precoder.

If we compare the performance of SVD in the unlimited feedback case and CSVD in the limited feedback case in figure 4.6, it can be seen that the unlimited feedback has a gain of about 0.3 dB over that of limited feedback. This could be viewed as the loss using limited feedback.

4.5 Summary of the results

The flow of our simulations is described and the corresponding results are presented. First of all, the SVD algorithm is tested to have gain in the case of no CS term and also small gain with CS term in equalization. For this reason, CSVD is then evaluated in the case of limited feedback. Several algorithms implementing CSVD are investigated. The one based on distance is proved to have no gain. The one based on phase shows a small gain in relatively low SNR range. Considering that channel estimation error affects the selection of precoders severely, preamble-based channel estimation is applied. It turns

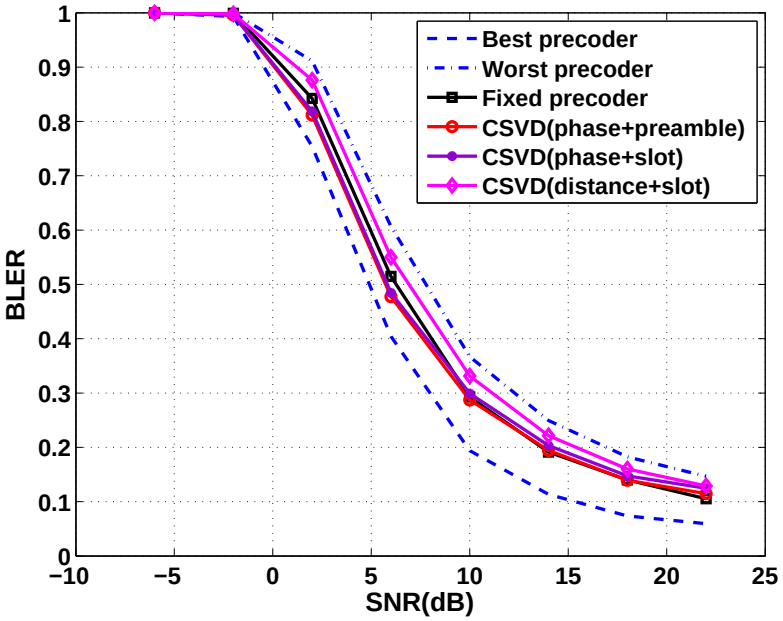

Figure 4.4: This figure shows performance comparison between the best/worst/fixed precoders and the precoder chosen by different proposed CSVD algorithms. CSVD based on distance shows no gain and CSVD based phase shows a small gain over fixed precoder in limited feedback case. Preamble-based CSVD using phase shows a relatively larger gain of 0.6 dB over fixed precoder when BLER equal to 0.5. See legend explanation in section 4.6 Explanation of the legends.

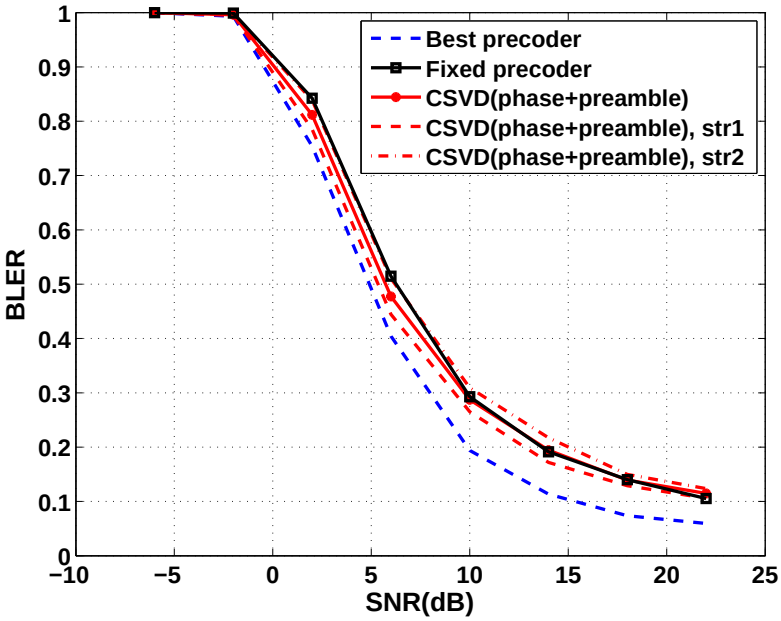

Figure 4.5: Preamble-based CSVD shows a clear difference on steam 1 and stream 2 in limited feedback case. See legend explanation in section 4.6 Explanation of the legends.

out to provide a considerable gain (0.6 dB at 0.5 BLER), especially on primary stream (around 1 dB gain over the secondary stream).

It is obvious that for all precoding methods implemented, there is always a cross point (around 10 dB SNR) with fixed precoder method. If we look into the reason for this, we could find some clues. In low SNR range, noise is the major factor that affects the performance of the system, while in high SNR range, data interference becomes the dominant factor. This is probably because that in the high SNR case, the channel estimation is affected largely not only by the data interference from the other steam, but also Inter-Symbol-Interference (ISI) caused by multiple paths. This kind of interference depends on both the real channel (the physical channel) and the data transmitted in current slot. Hence, the estimated channel should always contain both the real channel and the interference if perfect channel estimation is assumed.

In the case of slot based channel estimation, the channel estimation for the current slot is used for the next slot for precoding matrix decision. As explained in section "Channel estimation error", the data-caused interference varies among slots. The channel estimation of the previous slot can no longer evaluate the effect of interference for the current slot. As a result, the precoder chosen based on the channel estimation of previous slot cannot be as reliable as expected.

In the case of preamble based channel estimation, without regard to channel fading between slots in a frame, the estimated channel can still reconstruct the real channel

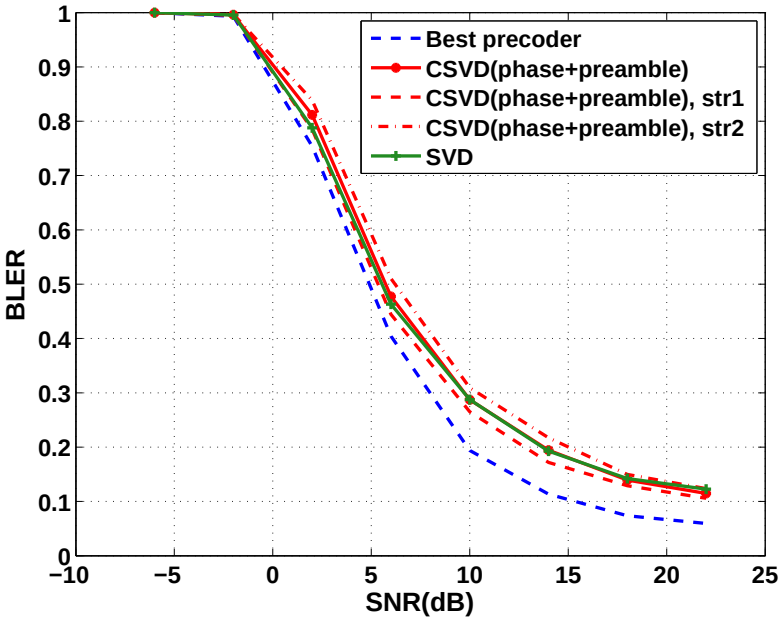

Figure 4.6: SVD with unlimited feedback has a gain of 0.3 dB compared with CSVD with unlimited feedback. See legend explanation in section 4.6 Explanation of the legends.

mostly. This makes the preamble-based CSVD to show gain in low SNR cases. However, as no interference is taken into account, the evaluation of the effective channel suffers from possible failure when SNR is high. That could be the reason of the high error floor. Also, in both cases, the performance will suffer from 5% probability of deep fading as described in the appendix "Simulator evaluation".

4.6 Explanation of the legends

Below is a list of legend explanation of simulation curves using different methods.

No precoding	Using no precoding matrix
Fixed precoder	Firstly randomly choose one of the four available precoders and then the selected one is used for precoding in all frames. For instance, if the second precoder is chosen, then all frames will use the second precoder for precoding
Best and worst precoder	Testing all four precoders for each channel realization and BER was calculated frame-wise, and the best and the worst performance for each channel realization was recorded, see eq.(4.3) and (4.4)
SVD	Using SVD decomposition for selection of precoder, see eq.(2.37)
CSVD(phase+preamble)	Using CSVD method judged by phase and using preamble for channel estimation, once per frame, see eq.(4.7)
CSVD(phase+slot)	Using CSVD method judged by phase and using pilots for channel estimation, once per slot, see eq.(4.7)
CSVD(distance+slot)	Using CSVD method judged by distance and using pilots for channel estimation, once per slot, see eq.(4.6)
str1, str2	Simulation results on stream 1 and stream 2, respectively

5

Discussion, conclusion and future work

In this thesis, several MIMO precoding algorithms are investigated in a WCDMA uplink MIMO simulator. Both unlimited feedback and limited feedback are investigated, aiming at finding an algorithm that improves system performance in the relatively low SNR region. All results are carried out from WCDMA standardized PA frequency-selective channel, and with CS method was chosen for the receiver equalization. This chapter gives the conclusion based on theory discussed in chapter 2 and the simulation results shown in chapter 4. Moreover, several suggestions are made for future work on this topic.

5.1 Discussion and conclusion

To deal with the crosstalk interference in a MIMO transmission, there are mainly two methods: using precoding to avoid crosstalk beforehand, or using equalization to suppress or cancel the crosstalk. These two methods can be implemented together. As studied with unlimited feedback situations, in the case of frequency selective transmission, a WCDMA MIMO system cannot avoid crosstalk completely with precoding only. However, theoretically, by implementing an appropriate equalization method in the receiver, precoding can improve the transmission performance.

In reality, there is a trade-off between the achievable gain and the algorithm complexity. As investivated in this thesis, while the CS method is used for equalization, a maximum gain of approximately 1.5 dB can be expected with the four standardized precoders at relatively low SNR as mentioned in chapter 4. This gain can only be obtained if the most suitable precoder is chosen for every transmission. Therefore, a method with high complexity will be less worthy to try, even if it can achieve the maximum possible gain.

In this thesis, an algorithm that we named as CSVD was tested, which is a way to implement SVD algorithm in the limited feedback condition. Phase was selected to be the key feature for evaluating the similarity between the SVD resulted precoder and the four standardized precoders. With relatively ideal channel estimation, this method has shown a considerable gain, and gives better performance on the primary stream, like the unlimited SVD method does. Nevertheless, since channel estimation can easily affect the performance of CSVD, it may not be a good idea to implement this algorithm straightly in the real product, unless more reliable estimation can be provided.

On the other hand, as discussed in chapter 4, it is a very significant property of CSVD that the primary stream gives better performance than the secondary stream. A real telecommunication system can probably benefit form this property, as it gives more reliable control channels. In addition, higher ordered modulation like 16-QAM can be implemented on the primary stream to increase the throughput, while the secondary stream keeps using low ordered modulation like Quadrature Phase Shift Keying (QPSK) to get more reliability. With this configuration, the overall performance of the system can hopefully be improved.

5.2 Future work

We suggest more studies on the effective channel. As the effective channel takes the precoding into account and shows how data streams are transmitted clearly, there should be some characteristic that can be found from it. If the significant feature can be abstracted from the effective channel coefficients, a good algorithm should be able to pick the most suitable precoder according to it. In this thesis, we have investigated the phase, power and orthogonality properties of the effective channel in several ways, but there was no meaningful result obtained. However, studying the relation between the effective channel and the precoder selection could be a good starting point for the future work.

We suggest more work on high SNR range. Though the study on relatively low SNR range has not given out very exciting results, simulation figures in chapter 4 has shown a potential gain from another point of view when SNR increased to a relatively high level. This gain can be considered as a possible improvement of the system maximum throughput. Thus, finding a suitable algorithm for the high SNR cases could be valuable, in order to give a user very high data rate in a perfect link condition.

We suggest studies on other scenarios. As discussed before, the receiver structure have a strong relation with precoding. Though not relevant to the current standardized and commercialized WCDMA system, other receiver structure like Vertical Bell Labs Layered Space-Time (V-BLAST) and equalization methods like IC could be valuable topic for some further studies [28]. In addition, though four precoders codebook is standardized already, it is interesting to see how much gain we can expect from adding more precoders. A simulation with eight precoders has been ran and only tiny difference can be seen comparing the maximum reachable gain with CS. Nevertheless, by trying

more precoders with other equalization methods and comparing the performances, a difference of maximum reachable gain can still be expected. This work is suggested in order to find a equalization method that is more suitable for precoded MIMO receiving procedure. Once a larger gain has been observed, more complex precoding algorithms will become worthy to test.

A

Simulator evaluation

A.1 A statistic result of PA channel deep fading

We evaluated the IT++ PA channel model with a simple simulation: no channel coding was used, the employed physical channels were DPDCH and DPCCH, and AWGN noise was disabled so that SNR can be considered as infinity. The receiver used was G-Rake with five fingers. A test of 100 frames were simulated to sketch the statistical characteristics of the channel model. The result is shown in figure A.1.

From the picture we can clearly see that though BER values are almost zero, there are cases that BER values are rather high (larger than 0.1). These cases, which we defined as deep fading cases, are caused by either huge channel attenuation or strongly

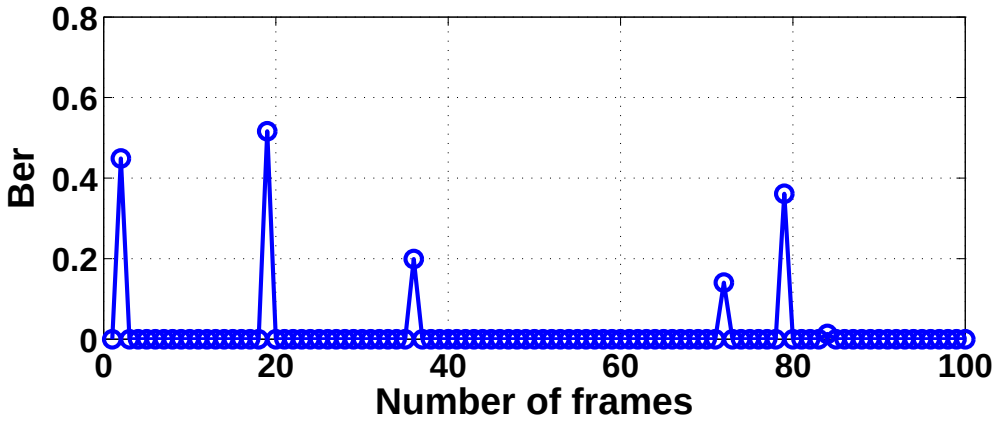

Figure A.1: Deep fading statistic result of the PA channel (SNR=∞). Peaks that higher than 0.1 denotes the deep fading cases.

destructive ISI. According to lots of repetitive simulation results (including the result shown in figure A.1), the probability that deep fading happens is about 5%.

To obtain this statistic result, a new channel realization is generated for each frame. It affects the system performance to some extent in high SNR cases.

A.2 Channel estimation error

We evaluated the channel estimation using Mean Absolute Percentage Error (MAPE) [29], i.e.,

$$\text{MAPE} = \frac{\frac{1}{L}\sum_{l=1}^{L}|\hat{h}(l) - \hat{h}|}{|\hat{h}|}. \tag{A.1}$$

For each SNR point 150 data points are collected. The MAPE is shown as a blue curve in figure A.2. Since there is no obvious characteristic can be abstract from the curves and the evaluation values are all under 10%, the channel estimation result can be considered reliable in terms of stability.

As discussed in the previous section, the channel is static for each frame, and the channel realizations that have seen by different frames are independent. Hence, the preamble that was defined in the section "3.3.8 Channel estimation" can be used for

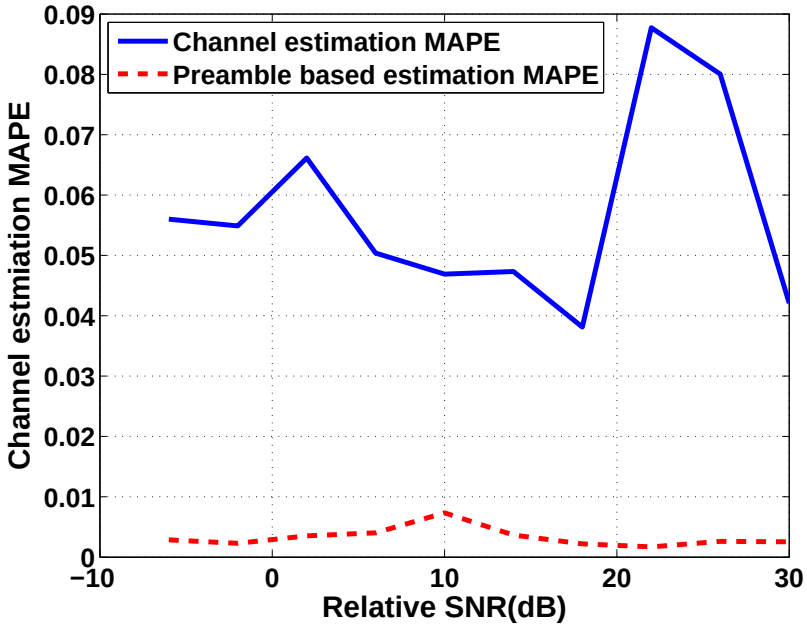

Figure A.2: MAPE of normal channel estimation. The preamble-based channel estimation is stable. Though the normal channel estimation MAPE shows some stochastic characteristic, the error percentage is kept pretty low. Hence the estimation result is reliable in terms of stability.

achieving better estimation on the channel. This channel estimation method that we defined as "preamble-based channel estimation", is to use the preamble transmitted before every frame for estimating the channel for the entire frame. The red dash line shown in the figure A.2 stands for the MAPE value of preamble-based channel estimation. Those MAPE values turned out to be very close to 0, which are much smaller than that of the generic slot-based channel estimation result shown by the blue curve. Hence, it is obvious that the channel estimation based on preamble is more reliable.

On the other hand, the channel estimation is inevitably affected by the interference from the data channels (E-DPDCH and S-E-DPDCH) since all are transmitted in the same physical channel. This conclusion can be drawn by comparing the two curves in figure A.2. In addition, the normal slot-based channel estimation curve shows a randomness, which shows that different contents of the data channels have different characteristics of interference. As a result, though the G-Rake receiver can evaluate the interference caused by data, the evaluation will not be suitable to the next slot and hence affects the precoding calculation. This problem is addressed as a motivation to the approach described in the section "4.4.3 Preamble-based CSVD".

A.3 G-Rake receiver performance evaluation

As G-Rake receiver uses extra fingers for interference suppression, the system should be able to achieve some gain in the overall performance comparing with a regular Rake receiver. To evaluate the performance of G-Rake, a simulation with 500 frames per SNR point were ran. Finger number was chosen as five, and the PA channel model was used for test. Both SISO and SIMO diversity model were tested, and Rake receiver is also simulated as a reference. The result is shown in figure A.3.

From the picture, it is obvious that G-Rake gives a much better performance than Rake (more than 5 dB gain). ISI is calculated by the extra fingers, and interference suppression is performed on the received signal, so that system achieved an obvious gain even though there is no inter-user-interference existing (G-Rake is supposed to be more effective in the case of multi-user communication [15]).

By adding one more antenna at receiver side, a SIMO diversity transmission model was formed. As expected, this model shown about 3 dB diversity gain comparing with G-Rake SISO, and the BLER floor was also decreased to be close to zero. According to the section "A.1 A statistic result of PA channel deep fading", there exists a possibility that one SISO link suffers from a deep fading and gives very high error rate. By implementing SIMO diversity, this kind of deep fading can be partly avoided, leading to a better average performance and a lower error floor.

A.4 SISO model evaluation

A comparison of some SISO simulation results with theoretical curves is shown in figure A.4 as a way to evaluate the simulator. The theoretical curves were generated by the MATLAB tool "BERTool" [30]. SNR range was selected to be from -2 dB to 14 dB, and

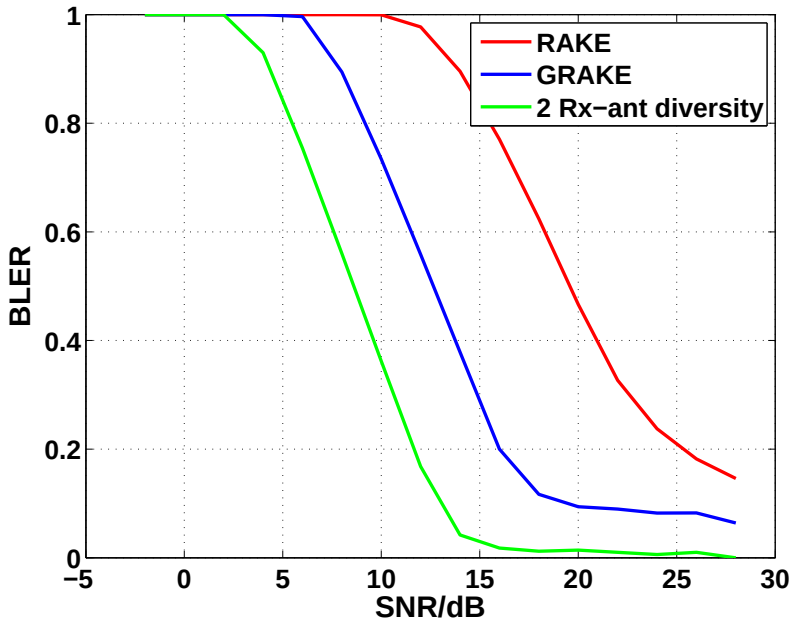

Figure A.3: Rake and G-Rake performance evaluation. It can be seen that G-Rake worked better than Rake. And comparing the G-Rake SIMO with G-Rake SISO, there is an obvious diversity gain (around 3dB).

the SISO simulation results were simulated with 9.6×10^5 data bits. AWGN channel and PA channel were tested without Turbo coding, and G-Rake receiver was used for the PA channel.

The figure shows that the simulated AWGN follows the theoretical AWGN curve perfectly in low SNR range. When SNR exceeds 9 dB, the BER value is approaching to the minimum possible BER value regarding the number of bits ($1/(9.6 \times 10^5) \approx 10^{-6}$). The BER value goes below the theoretical curve when SNR equals to 10. Afterwards, the BER values become zero. This comparison shows that the AWGN SISO link is ready for the further tests. Since this comparison result conformed the expected system behavior, the simulator with G-Rake can be considered reliable as well.

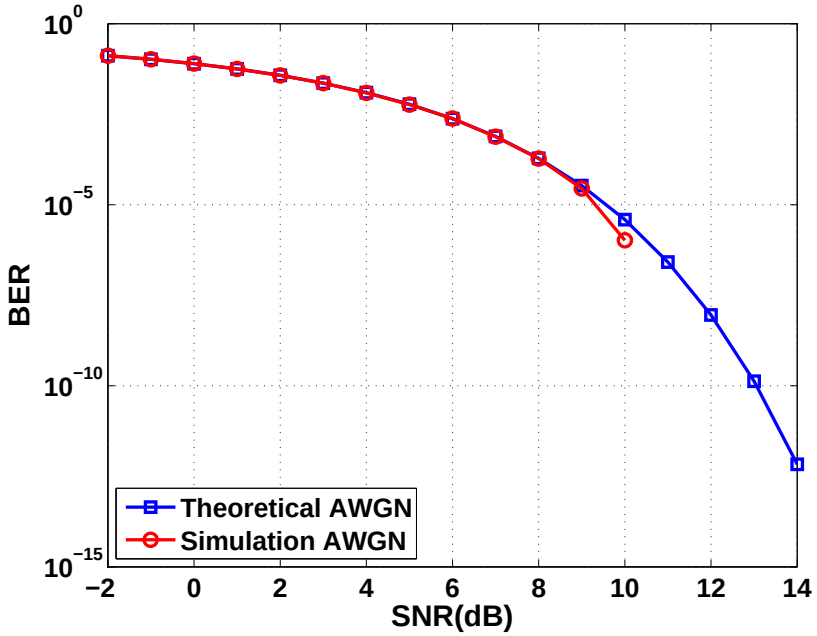

Figure A.4: Comparison of simulation results and theoretical curves, where the AWGN simulation result fits the theoretical curve pretty well.

B

Acronyms

1G First-Generation

2G Second-Generation

3G Third-Generation

3GPP the Third Generation Partnership Project

4G Forth-Generation

5G Fifth-Generation

AWGN Additive White Gaussian Noise

BER Bit Error Rate

BLER Block Error Rate

BPSK Binary Phase Shift Keying

CDMA Code Division Multiple Access

CS Crosstalk Suppression

CSVD Closest-to-SVD

DL Downlink

DPCCH Dedicated Physical Control Channel

DPDCH Dedicated Physical Data Channel

DS-CDMA Direct-Sequence CDMA

DSSS Direct-Sequence Spread Spectrum

E-DPCCH Enhanced Dedicated Physical Control Channel

E-DPDCH Enhanced Dedicated Physical Data Channel

EGC Equal-Gain Combining

FBI Feedback Information

FDMA Frequency Division Multiple Access

G-Rake Generalized Rake

GSM Global System for Mobile communication

HARQ Hybrid Automatic Repeat Request

IC Interference Cancellation

IS-95 Interim Standard 95

IMT-2000 International Mobile Telecommunications for the year 2000

ISI Inter-Symbol-Interference

ITU International Telecommunication Union

i.i.d. independent and identically distributed

LOS Line Of Sight

LTE long Term Evolution

M-**QAM** M-ary Quadrature Amplitude Modulation

MAP Maximum a Posteriori

MAPE Mean Absolute Percentage Error

MIMO Multiple-Input Multiple-Output

MISO Multiple-Input Single-Output

ML Maximum Likelyhood

MMSE Minimum-Mean-Squared-Error

MRC Maximum Ratio Combining

OVSF Orthogonal Variable Spreading Factor

PA Pedestrian A

QPSK Quadrature Phase Shift Keying

QoS Quality of Service

RRC Root Raised Cosine

S-DPCCH Secondary Dedicated Physical Control Channel

S-E-DPCCH Secondary Enhanced Dedicated Physical Control Channel

S-E-DPDCH Secondary Enhanced Dedicated Physical Data Channel

SC Selection combining

SF Spreading Factor

SIMO Single-Input Multiple-Output

SINR Signal-to-Interference-plus-Noise Ratio

SISO Single-Input Single-Output

SNR Signal to Noise Ratio

SU-MIMO Single User MIMO

SVD Singular Value Decomposition

TDL Tapped Delay Line

TDMA Time-Division Multiple-Access

TFCI Transport Format Combination Indicator

TPC Transmission Power Control

UE User Equipment

UL Uplink

UMTS Universal Mobile Telecommunications System

V-BLAST Vertical Bell Labs Layered Space-Time

WCDMA Wideband Code Division Multiple Access

ZF Zero-Forcing

C

List of symbols

$a_{k,i}(l)$	spreading waveform
$\mathbf{c}$	chip sequence
$\{c_{k,i}(l)\}_{l=1}^{N}$	chip set
C_i	the capacity of the ith stream
D	distance between precoders
D_{phase}	distance in phase between precoders
F	finger number
$\mathbf{g}$	RAKE combining weight
h	constant channel coefficient
$h(t)$	time variant channel coefficient
$h(t,\tau)$	TDL channel coefficient
$h(l)$	the channel realization for the lth transmission sample
$\hat{\mathbf{h}}$	tap-based channel estimation
$\mathbf{H}$	channel coefficient matrix
$\hat{\mathbf{H}}$	channel estimation matrix
$\hat{\mathbf{H}}_{\text{eff}}$	effective channel estimation matrix
$\hat{\mathbf{h}}_{\text{eff}}$	effective channel estimation vector
$\mathbf{h}_i$	channel coefficient for the ith stream
$\hat{h}(l)$	the channel estimation coefficient for the lth sample
$\hat{h}$	average channel estimation coefficient

$h_l(t)$	channel coefficient for the lth path
i	symbol index
$\mathbf{I}$	identity matrix
k	stream index
L	resolvable multipaths number
$m_{k,i}(t)$	the ith BPSK symbol of the kth data stream
$MMSE_i$	minimum mean-square-error value of the ith stream
$n(t)$	AWGN noise
$\mathbf{n}$	a vector of i.i.d. AWGN noise
N	spreading factor
$p_{\text{rect}}(t)$	rectangular pulse
$p(t)$	general pulse shape
P	a set of precoders, or codebook
$\mathbf{r}$	despread symbol sequence
$\mathbf{R}$	impairment correction matrix
$r_{k,i}(t)$	the despread ith symbol of the kth data stream
R_u	covariance matrix
RF	roll-off factor
$s_{k,i}(t)$	spread signal of the ith symbol of the kth data stream
$\tilde{s}(t)$	precoded transmission signal
$\mathbf{s}$	a set of sample of transmitted signal
$s_p(t)$	the transmitted pilot signal
$s_p(q)$	the lth sample of the transmitted pilot signal
$\mathbf{s}_p$	pilot vector
$SINR_i$	signal-to-interference-plus-noise ratio
t	time
T_s	symbol duration
T_c	chip duration
u	overall noise
$\mathbf{U}, \mathbf{V}$	SVD generated unitary matrix
w	complex precoding weight
$\mathbf{W}$	precoding matrix
$\mathbf{y}$	a set of samples of received signal

$y_{k,i}(t)$	received signal of the ith symbol of the kth data stream
$\tilde{y}(t)$	received signal
$\tilde{y}(t,\tau)$	TDL received signal
$\tilde{y}_p(t)$	the received pilot signal
$\tilde{y}_p(l)$	the lth sample of received pilot signal
$\mathbf{z}$	Rake combined symbol sequence
$\delta(t)$	Dirac delta function
ε	the average channel estimation error
$\varepsilon(q)$	the channel estimation error for the lth sample
ρ	SVD generated singular value
σ_a^2	variance of noise
σ_y^2	variance of the received signal
Σ	SVD generated singular value matrix
τ	delay
τ_l	the delay of the lth path
ϕ	phase angle of a corresponding precoding weight

D

List of notations

$\mathrm{E}\{\cdot\}$	expectation
$\mathrm{tr}\{\cdot\}$	trace of a matrix
$\phi(\cdot)$	phase of a complex number
$\mathbf{A}^H$	Hermitian transpose of matrix A
$\mathbf{A}^T$	transpose of matrix A
$\mathbf{A}^*$	conjugate of matrix A

E

List of parameters

E.1 System parameters

Modulation type	BPSK combined QPSK
Number of antennas in MIMO	2×2
Number of predefined precoder	4
Receiver structure for TDL	G-Rake

E.2 Physical channel parameters

Data bits per DPDCH frame	3196
Data bits per E-DPDCH frame	19176
Symbol number of DPDCH	9600
Symbol number of E-DPDCH	57600
Slots per frame	15
Pilot length	10

E.3 Turbo and interleaver parameters

Turbo coding rate	1/3
Codeword length	9600
Constraint length	4
Turbo interleaver length	3196
Polynomials generator	013, 015
Decoding method	LOGMAX
Block interleaver dimension	4×4

E.4 Spreading parameters

DPDCH spreading factor	4
E-DPDCH spreading factor	2,2,4,4
DPCCH spreading factor	256
Chips per slot	2560
Chips per frame	38400
Chip duration (s)	260.4×10^{-9}
Chip rate (Mcps)	3.84

E.5 Pulse shape parameters

Pulse shape	RRC
Filter length	6
Up-sampling rate	8
Roll-off factor	0.22
Sample time (s)	$32.55 \times 10^{-}9$

E.6 PA channel parameters

Doppler	10^{-28} s
Number of taps	4
Tap location (μs)	0.0 0.110 0.190 0.410
Tap power (dB)	0.0 -9.7 -19.2 -22.8

E.7 G-Rake parameters

Number of fingers	5
Combining method	MRC

Bibliography

[1] P. Sharma, "Evolution of Mobile Wireless Communication Networks-1G to 5G as well as Future Prospective of Next Generation Communication Network ," *Computer Science and Information Technology*, vol. 2, pp. 47–53, 2013.

[2] D. Gilstrap, "Ericsson Mobility Report," ERICSSON, Tech. Rep., November 2013.

[3] H. Holma and A. Toskala, Eds., *WCDMA for UMTS - Radio Access For Third Generation Mobile Communications.* John Wiley and Sons, LTD, 2001, revised edition.

[4] J. Wannstrom. HSPA. [Online]. Available: http://www.3gpp.org/technologies/keywords-acronyms/99-hspa

[5] 3GPP. 3GPP feature and study item list. [Online]. Available: http://www.3gpp.org/DynaReport/FeatureListFrameSet.htm

[6] C. Oestges and B. Clerckx, *MIMO Wireless Communications.* Cambridge University Press, 2007.

[7] C. B. Peel, B. M. Hochwald, and A. L. Swindlehurst, "A vector-perturbation technique for near-capacity multiantenna multiuser communication-Part I: channel inversion and regularization," *IEEE Trans. Coms.*, vol. 53, no. 1, pp. 195–202, 2005.

[8] C. Masouros and E. Alsusa, "Selective channel inversion precoding for the downlink of MIMO wireless systems," in *IEEE ICC 2009 proceedings.* IEEE Communications Society, 2009.

[9] C. Li and X. Wang, "Performance comparisons of MIMO techniques with application to WCDMA systems," *EURASIP Journal on Applied Signal Processing*, vol. 5, pp. 649–661, 2004.

[10] A. Goldsmith, *Wireless Communications.* Cambridge University Press, 2005.

[11] W. Zhuang and W. V. Huang, "Phase precoding for frequency-selective Rayleigh and Rician slowly fading channels," *IEEE transactions on vehicular technology*, vol. 46, no. 1, February 1997.

[12] H. R. Bahrami and T. Le-Ngoc, "MIMO precoder designs for frequency-selective fading channels using spatial and path correlation," *IEEE transactions on vehicular technology*, vol. 57, no. 6, November 2008.

[13] D. J. Love, R. W. Health, and W. Santipach, "What is the value of limited feedback for MIMO channels," *Communications Magazine, IEEE*, vol. 42, 2004.

[14] Doxygen. (2013, July) IT++ documentation. [Online]. Available: http://itpp.sourceforge.net/4.3.1/

[15] G. E. Bottomley, T. Ottosson, and Y.-P. E. Wang, "A Generalized Rake receiver for interference suppression," *IEEE Journal on Selected Areas in Communications*, vol. 18, no. 8, 2000.

[16] S. Shenoy, I. Ghauri, and D. Slock, "Optimal precoding and MMSE receiver designs for MIMO WCDMA," *Vehicular Technology Conference, 2008. VTC Spring 2008. IEEE*, pp. 893–897, 2008.

[17] T. Heikkilä, "Rake receiver," Teliasonera, Tech. Rep., 2004.

[18] A. Goldsmith, S. A. Jafar, N. Jindal, and S. Vishwanath, "Capacity limits of MIMO channels," *Selected Areas in Communications*, vol. 21, pp. 684–702, 2003.

[19] L. C. Godara, "Part ii: Beamforming and direction of arrival considerations," in *Application to antenna arrays to mobile communications*, 1997, pp. 1195–1247.

[20] V. Tarokh, H. Jafarkhani, and A. R. Calderbank, "Space-Time Block Codes from Orthogonal Designs," *IEEE transactions on information theory*, vol. 45, no. 1, July 1999.

[21] Q. H. Spencer, A. L. Swindlehurst, and M. Haardt, "Zero-forcing methods for downlink spatial multiplexing in multiuser MIMO channels," *IEEE transactions on signal processing*, vol. 52, no. 461-471, Feb 2004.

[22] U. Madhow, *Fundamentals of Digital Communication.* Cambridge University Press, 2008.

[23] T. Haustein, C. von Helmolt, E. Jorswieck, V. Jungnickel, and V. Pohl, "Performance of MIMO systems with channel inversion," *55th IEEE Veh. Technol. Conf. (VTC)*, vol. 1, pp. 35–39, May 2002.

[24] S. J. Grant, K. J. Molnar, and G. E. Bottomley, "Generalized Rake receivers for MIMO systems," in *Vehicular Technology Conference*, vol. 1. IEEE, 2003, pp. 424–428.

[25] 3GPP. 3GPP specifications. [Online]. Available: http://www.3gpp.org/DynaReport/21801.htm

[26] E. Dahlman, S. Parkvall, J. Sköld, and P. Beming, *3G Evolution - HSPA and LTE for Mobile Broadband*, 1st ed. Academic Press, 2007.

[27] R. des Lucioles Sophia Antipolis, "3GPP TR 25.890," 3rd Generation Partnership Project, Tech. Rep., 2005.

[28] C. Shen, Y. Zhu, S. Zhou, and J. Jiang, "On the performance of V-BLAST with zero-forcing successive interference cancellation receiver," *IEEE Communications Society*, 2004.

[29] R. A. Yaffee and M. McGee, *Introduction to time series analysis and forecasting : with applications of SAS and SPSS*. San Diego Academic Press, 2000.

[30] MathWorks. Open bit error rate analysis GUI (BERTool). The MathWorks, Inc. [Online]. Available: http://www.mathworks.se/help/comm/ref/bertool.html